



Università degli Studi Mediterranea di Reggio Calabria
Archivio Istituzionale dei prodotti della ricerca

Evaluating the effects of forest tree species on rill detachment capacity in a semi-arid environment

This is the peer reviewed version of the following article:

Original

Evaluating the effects of forest tree species on rill detachment capacity in a semi-arid environment / Parhizkar, M.; Shabanpour, M.; Miralles, I.; Cerda, A.; Tanaka, N.; Asadi, H.; Lucas-Borja, M. E.; Zema, D. A.. - In: ECOLOGICAL ENGINEERING. - ISSN 0925-8574. - 161:106158(2021). [10.1016/j.ecoleng.2021.106158]

Availability:

This version is available at: <https://hdl.handle.net/20.500.12318/90127> since: 2024-11-20T10:07:42Z

Published

DOI: <http://doi.org/10.1016/j.ecoleng.2021.106158>

The final published version is available online at: <https://www.sciencedirect.com>.

Terms of use:

The terms and conditions for the reuse of this version of the manuscript are specified in the publishing policy. For all terms of use and more information see the publisher's website

Publisher copyright

This item was downloaded from IRIS Università Mediterranea di Reggio Calabria (<https://iris.unirc.it/>) When citing, please refer to the published version.

(Article begins on next page)

1 *This is the peer reviewed version of the following article:*

2
3 ***Parhizkar, M., Shabanpour, M., Miralles, I., Cerdà, A., Tanaka, N., Asadi, H., ... &***
4 ***Zema, D. A. (2021). Evaluating the effects of forest tree species on rill detachment***
5 ***capacity in a semi-arid environment. Ecological Engineering, 161, 106158,***

6
7 *which has been published in final doi*

8
9 10.1016/j.ecoleng.2021.106158

10
11
12 (<https://www.sciencedirect.com/science/article/pii/S0925857421000124>)

13
14 *The terms and conditions for the reuse of this version of the manuscript are specified in the*
15 *publishing policy. For all terms of use and more information see the publisher's website*

16 **Evaluating the effects of forest tree species on rill detachment capacity in a semi-arid**
17 **environment**

18
19 *Misagh Parhizkar*¹, *Mahmood Shabanpour*¹, *Isabel Miralles*², *Artemio Cerdà*³, *Nobuaki*
20 *Tanaka*⁴, *Hossein Asadi*⁵, *Manuel Esteban Lucas-Borja*⁶, *Demetrio Antonio Zema*^{7,*}

21
22 ¹ Faculty of Agricultural Sciences, University of Guilan, 41635-1314 Rasht, Iran

23 ² Department of Agronomy & Center for Intensive Mediterranean Agrosystems and Agri-
24 food Biotechnology (CIAIMBITAL), University of Almeria, E-04120, Almería, Spain.

25 ³ Soil Erosion and Degradation Research Group (SEDER), University of Valencia, E-
26 46001 Valencia, Spain

27 ⁴ Ecohydrology Research Institute, The University of Tokyo Forests, Graduate School of
28 Agricultural and Life Sciences, The University of Tokyo, Seto, Japan

29 ⁵ Department of Soil Science, University of Tehran, 11369 Tehran, Iran

30 ⁶ Escuela Técnica Superior Ingenieros Agrónomos y Montes, Universidad de Castilla-La
31 Mancha, Campus Universitario, E-02071 Albacete, Spain

32 ⁷ Department AGRARIA, Mediterranean University of Reggio Calabria, Loc. Feo di Vito,
33 I-89122 Reggio Calabria, Italy

34

35 * Correspondence: dzema@unic.it

36

37 **Abstract**

38

39 The beneficial effects of plant roots in decreasing soil detachment in forest ecosystems
40 exposed to rill erosion are well known. However, these effects vary largely between
41 different plant species. There has been lots of research into the relationship between root-
42 soil systems and rill erodibility with a particular focus on grass species. Conversely, fewer
43 studies are available for tree species, especially in forests of semi-arid or arid environments.
44 Greater knowledge is therefore needed to identify the most effective tree species against rill
45 erosion in these ecosystems, where water availability is the limiting factor for vegetation
46 growth and afforestation is often the only solution to control erosion. To fill this gap, this
47 study evaluates the rill detachment capacity of soils with four tree species (*Parrotia*
48 *persica*, *Carpinus betulus*, *Quercus castaneifolia*, and *Pinus taeda*) in a semi-arid forest
49 ecosystem in Northern Iran. These species are typical of these forests, but they also grow in
50 other environmental contexts. The rill detachment was simulated in a laboratory flume at

51 five slope gradients (1% to 5%) and five flow rates (0.22 to $0.69 \text{ L m}^{-1} \text{ s}^{-1}$) on soil samples
52 with each of the tree species. The specific goal of the study was to evaluate which tree
53 species with its specific root characteristics is most effective at reducing the rill detachment
54 capacity. Moreover, simple prediction models are proposed to evaluate if it is possible to
55 estimate the rill detachment capacity and rill erodibility (K_r) from the unit stream power for
56 the investigated tree species. The soils with *Parrotia persica* and *Carpinus betulus* showed
57 the lowest and the highest rill detachment capacity, respectively. The higher root system
58 biomass of *Parrotia persica* could have played a binding effect on the soil, thus improving
59 its aggregate stability thanks to the action of plant's root system. Based on these results,
60 *Parrotia persica* is able to provide a higher soil protection capacity against erosion
61 compared to the other tree species. A logarithmic function was accurate in predicting the
62 rill detachment capacity from the unit stream power at water flow rates over 0.0025 m s^{-1} .
63 By a regression between the rill detachment capacity and the shear stress of the soil, rill
64 erodibility and critical shear stress of soils were estimated for the four tree species; the rill
65 erodibility and critical shear stress are important input parameters for physically-based
66 erosion models. Overall, the results of this study can support land planners in the choice of
67 tree species most indicated for soil conservation as well as in the extensive application of
68 erosion prediction models.

69

70 **Keywords:** forest; *Parrotia persica*; rill erodibility; unit stream power; root density;
71 shallow flow; soil erosion.

72

73 **1. Introduction**

74

75 Soil erosion is a complex environmental process, consisting of detachment from place,
76 transport, and deposition of soil particles, often at a long distance (Ellison, 1947;
77 Prosdocimi et al., 2016). Soil detachment is due to rainsplash and overland flow (Govers et
78 al., 1990), which are the main soil detachment mechanisms in inter-rill and rill erosion,
79 respectively (Zhang et al., 2003). Regarding rill erosion, its maximum value at zero
80 sediment concentration is called "soil detachment capacity" (Foster, 1982). This is the most
81 important parameter driving soil resistance to water erosion, particularly on steep slopes
82 (Wang et al., 2018b; Owoputi and Stolte, 1995). Regarding concentrated flow erosion, this
83 process is driven by "soil detachment capacity by rill flow" or, more simply, "rill
84 detachment capacity" (hereinafter indicated by " D_c "). Therefore, it is essential to quantify

85 which factors influence soil detachment capacity, in order to control and limit erosion by
86 appropriate soil management practices. In general, these practices are based on increasing
87 vegetal cover and/or modifying soil properties (Cerdà et al., 2016).

88 For technical, economic or legal reasons, it is not always easy to modify soil properties.
89 The use of vegetation with tree or herbaceous species is a more viable solution to control
90 surface erosion on hillslopes, reducing the soil erodibility. Revegetation for erosion control
91 is based on the effects of the above-ground biomass; the latter, however, can temporally
92 disappear, because of fire, overgrazing or concentrated erosion, particularly in arid and
93 semi-arid areas (De Baets et al., 2007). In these environments, the importance of below-
94 ground biomass that can effectively control soil erosion rates is often neglected. The
95 beneficial effects of an extensive vegetal cover against soil erosion are many: the reduction
96 of surface runoff volume and velocity (Fiener and Auerwald, 2003; Koskiaho, 2003; Li et
97 al., 2013), the increase in water infiltration (De Baets et al., 2008; Li et al., 1992; 1995),
98 and bonding of soil particles at the soil surface (De Baets et al., 2006; 2007). Most of these
99 effects are due to the plant root system and are essential, particularly on steep slopes and
100 with loose soils, since plant roots reduce the sediment detachment by increasing the shear
101 strength of the root-soil matrix (Abdi et al., 2010; Herbrich et al., 2018; Wang et al.,
102 2018a). However, these effects vary largely depending on the different characteristics of the
103 vegetation (tree, shrub or, grass layer; plant species; environmental conditions) (Jiao et al.,
104 2008), and particularly on the size, distribution and density of the plant roots (De Baets et
105 al., 2007b; Gyssels et al., 2005). Based on the characteristics of the root system, the most
106 suitable plant species for erosion control can be properly selected to achieve a reduction in
107 soil erosion (Pollen, 2007). Among the root system characteristics, the root system biomass
108 (that is, the dry mass of roots in the soil) has been used by many authors as a key driver in
109 reducing soil detachment (Wang et al., 2014b; Li et al., 2015; Wang et al., 2018a; 2018b;
110 Parhizkar et al., 2020b). For example, Wang et al. (2014a; 2014b) found that root density is
111 the most influential factor on soil detachment capacity because of its physical and chemical
112 binding effects (De Baets et al., 2006; Zhang et al., 2013). De Baets et al. (2007) showed
113 that root density is correlated to soil detachment rate by a negative exponential equation.
114 Unfortunately, information on the effects of plant roots on topsoil resistance to rill erosion
115 is not sufficient (De Baets et al., 2007). A large variety of tree species exist, and each
116 species has its own specific root system characteristics. Previous studies have demonstrated
117 that different tree species exert different influences on the physico-chemical properties of
118 soils (e.g., Gyssels et al., 2005; Meek et al., 1992; Keller and Håkansson, 2010; Gyssels

119 and Poesen, 2003; Shabanpour et al., 2020), but particularly on soil detachment capacity
120 (Wang et al, 2014a; Zhang et al, 2013; Mamo and Bubenzer, 2001a; 2001b).

121 The studies that have evaluated the effects of plant root systems on soil erodibility and rill
122 detachment capacity have been carried out in specific environments (e.g., Loess Plateau in
123 China, Wang et al., 2014b; 2018a) and at the landscape scale (e.g., Li et al., 2015; Geng et
124 al., 2021, again in Loess Plateau) or have mainly focused on shrub and grass species (e.g.,
125 De Baets et al., 2006; Zhang et al., 2013; Wang et al., 2021). In general, all these studies
126 have highlighted that the detachment rate of rooted soils is reduced compared to other
127 soils, with consequent increased soil stability (e.g., Mamo and Bubenzer 2001a; 2001b),
128 since erodibility is greatly reduced (even by more than 80-90%) compared to bare or
129 deforested soils (Wang et al., 2014a; Parhizkar et al., 2020b).

130 Some authors have also demonstrated that the effects of plant roots on soil erosion vary
131 depending on the plant species (Wang et al., 2018b) and the hydraulic parameters of the
132 water flow and soil properties (Gyssels et al., 2005). Despite this large body of literature,
133 less attention has been paid to tree species and, especially, to forest ecosystems, which, in
134 some environmental contexts (steep slopes and arid or semi-arid climate) may be
135 particularly prone to rill erosion. In fact, rill erosion is the most important erosive process
136 on hillslopes with a high gradient (Wang et al., 2014b; Owoputi et al., 1995), and semi-arid
137 and arid climates - such as the Mediterranean Basin - are characterized by heavy
138 rainstorms, resulting in highly concentrated runoff rates with high erosion power (Fortugno
139 et al., 2017). Forest cover with trees that have a well-developed root system is highly
140 effective at reducing soil erosion (Gyssels et al., 2005; Parhizkar et al., 2020b). Moreover,
141 afforestation with tree species is often the only solution for reducing soil erosion in arid or
142 semi-arid ecosystems, where water availability is the limiting factor for vegetation growth
143 (Querejeta et al., 2001). Therefore, more research is needed to understand how a given
144 forest tree species with a root system having specific biomass characteristics drives the soil
145 detachment process. In other words, there is a need to evaluate the soil detachment capacity
146 under an individual plant species and different soil and hydraulic conditions. Such
147 evaluations are useful to select the most effective tree species for afforestation in steep
148 hillslopes with high erosion rates (Norris et al., 2008; Perez et al., 2017).

149 To fill these gaps, this study quantifies the rill detachment capacity in soils sampled under
150 four species of adult trees (*Parrotia persica*, *Quercus castaneifolia*, *Pinus taeda* and
151 *Carpinus betulum*) in Saravan Forest Park (Northern Iran), using an experimental flume.
152 Moreover, simple models are proposed for the specific environmental conditions and tree

153 species, to predict the soil detachment capacity and rill erodibility. This investigation adds
154 the effect of the plant components to the results of a previous study by Parhizkar et al.
155 (2020a), carried out at the landscape scale under the same experimental conditions. These
156 authors showed that: (i) the soil detachment capacity of concentrated flow is lower in
157 forests and woodlands compared to grasslands and croplands; (ii) the unit stream power of
158 water flow is a very accurate predictor of soil detachment capacity. Following this
159 approach, our research questions were the following: (i) Which tree species with its specific
160 root system is more able to reduce the rill detachment capacity?; (ii) Are the prediction
161 models proposed by Parhizkar et al. (2020a) also valid at a smaller scale for the analyzed
162 tree species?

163

164 **2. Materials and methods**

165

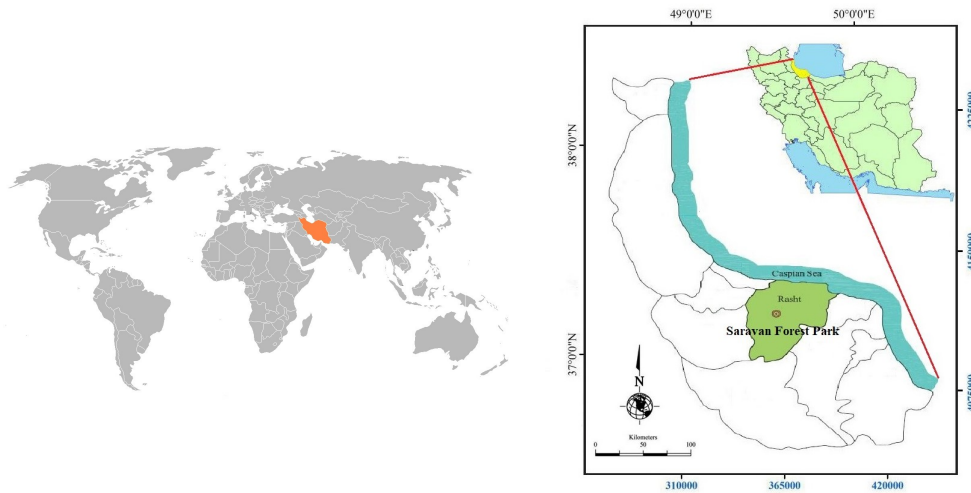
166 *2.1. Study area*

167

168 The province of Guilan (Northern Iran) lies between the southern coast of the Caspian Sea
169 and the northern part of the Alborz Mountains. The landscape of this province consists of a
170 green belt of old-growth Hyrcanian forests with high diversity of tree species and plant
171 communities (Amoopour et al., 2016). According to Parhizkar et al. (2020a), special
172 attention must be paid to the forests of this province, where existing problems of erosion
173 may increase if soil conservation issues are neglected.

174 The experimental site is located in Saravan Forest Park, which is one of the oldest forests in
175 Guilan province (outlet coordinates 37°08'04" N, 49°39'44" E). The park drains the Saravan
176 watershed (coordinates 37°08'04" N, 49°39'44" E), which covers an area of 14.87 km² at an
177 elevation from 50 to 250 m (Figure 1).

178



(a)



(b)

179

180 Figure 1 - Geographical location (a) (source: Google Earth, 2020) and aerial map (b) in the
 181 study area (Saravan Forest Park, Northern Iran).

182

183 This area has a Mediterranean climate, *Csa* type, according to the Köppen–Geiger
 184 classification (Kottek et al., 2006). The mean annual precipitation and temperature are 1360
 185 mm and 16.3 °C, respectively (IRIMO, 2016); precipitation is mainly concentrated in the
 186 coldest months and scarce in the dry period (Figure 1(SD)).

187 The Saravan watershed features an abundant biodiversity of forest plants, including 80 tree
 188 and shrub species (Sagheb-Talebi, et al., 2005; Hosseini, 2003, Kartoolinejad, et al., 2007).
 189 The dominant tree species are *Carpinus betulus* L. (*C. betulus*), *Quercus castaneifolia*
 190 C.A.Mey. (*Q. castaneifolia*), *Pinus taeda* L. (*P. taeda*), and *Parrotia persica* C.A.Mey. (*P.*
 191 *persica*) (Picchio et al., 2020; Mirabolfathy et al., 2018; Payam and Pourrajabali, 2020;
 192 Karimi et al., 2018). These species are typical of Northern Iran but grow throughout the
 193 Southern Caspian area (*P. persica* and *Q. castaneifolia* are also well diffused in Turkey and
 194 Azerbaijan), South-eastern United States (*P. taeda*), and Western Asia and Central,
 195 Eeastern, and Southern Europe (*C. betulus*). Other shrub and herbaceous species in the area

196 are *Artemisia annua* L., *Cynodon dactylon* (L.) Pers., *Hedera helix* L., *Hedera pastuchovii*
 197 *Woron. Ex Grossh.*, *Hypericum androsaemum* L., *Hypericum perforatum* L., *Juncus*
 198 *bufonius* L., *Juncus glaucus* Ehrh., *Mentha pulegium* L., *Morus alba* L., *Primula*
 199 *heterochoroma* Starf., *Prunus domestica* L., *Scutellaria albida* L., and *Solanum dulcamara*
 200 L.

201 Regarding the tree species, *P. persica* is a deciduous tree from Hamamelidaceae family,
 202 specifically native tonorthern Iran (Sefidi et al., 2011; Karimi et al., 2018). This is a highly
 203 ornamental tree or large shrub that can grow at an altitude of 20-25 m and tolerates drought,
 204 heat, wind and cold (Gilman, 2014). *C. betulus* is a semi-shade tolerant species (Marvie-
 205 Mohadjer, 2019), while *P. taeda* is an exotic and fast growing coniferous species (Picchio
 206 et al., 2020), which is used for commercial plantations. *Q. castaneifolia* is one of the most
 207 important native oak species of Iran (Payam and Pourrajabali, 2020). Table 1 showsthe
 208 main physiological characteristics of these tree species surveyed in the study area.

209

210 Table 1 – Main physiological characteristics (mean ± std. dev.) of the forest tree species
 211 surveyed in the study area (Saravan Forest Park, Northern Iran).

212

Tree species	Height (m)	Diameter^(*) (m)	Cover (%)
<i>Parrotia persica</i>	19 ± 0.6	0.57 ± 0.03	40
<i>Pinus taeda</i>	16 ± 0.3	0.26 ± 0.03	30
<i>Carpinus betulus</i>	22 ± 0.7	0.60 ± 0.04	15
<i>Quercus castaneifolia</i>	23 ± 0.7	0.61 ± 0.04	15

213 Note: (*) measured in this study at breast height.

214

215 Four mixed forests, with *C. betulus*, *Q. castaneifolia*, *P. taeda* and *P. persica* as prevalent
 216 species in areas with the same slope gradient were selected for this study (Abedi and
 217 Pourbabaei, 2011; Amoopour et al., 2016). On average, the *C. betulus* and *Q. castaneifolia*
 218 species each cover 15% of the area, while *P. persica* and *P. taeda* are the dominant species
 219 on 40% and 30% of the total area, respectively (Table 1). All the species are less than 15-20
 220 years old. *P. persica* shows a fibrous root system growing horizontally in the soil (Abdi et
 221 al., 2014). By contrast, *Q. castaneifolia*, *P. taeda*, and *C. betulus* have deep taproot
 222 systems, and their roots grow vertically along the soil profile (Hacke et al., 2000; Rewald et
 223 al., 2016; Abdi and Deljouei, 2019). *C. betulus* has the largest and deepest root system with

224 the coarsest root diameter (Kooch et al., 2016; Bonyad, 2006). About ten years ago, some
225 of the hillslopes in Saravan Park were deforested to install high-voltage electricity pylons,
226 with high density tree and plant cover being totally removed (Parhizkar et al., 2020b). This
227 deforestation induced intense rill erosion (Figure 2), meaning management action is
228 absolutely necessary to avoid further biodiversity losses.
229



230

231

(a)

(b)

232 Figure 2 - Views of rill erosion on hillslopes with previous cover of *Quercus castaneifolia*
233 after deforestation (Saravan Forest Park, Northern Iran) - (a, aerial view using a drone, and
234 b, front view).

235

236 2.2. Soil sampling procedure

237

238 To measure the rill detachment capacity of the soil (D_c), between October and November
239 2019 undisturbed samples were collected in each of the areas with a dominant species
240 among *P. persica*, *P. taeda*, *C. betulus*, and *Q. castaneifolia*. Five samples were collected
241 around five trees for each species. For each tree, two quadrats (1 x 1 m and 2 x 2 m) were
242 overlaid on the ground. Two samples were collected in the vertices of the diagonal of the
243 first quadrat, and two others were collected in the vertices of the opposite diagonal of the
244 second quadrat. The fifth sample was collected immediately beside the trunk. This design
245 allowed sampling in different positions (two opposite diagonals) and three distances from
246 the tree (0, 0.7 and 1.4 m).

247 The sampling procedure, adapted to this study from the works of Zhang et al. (2003; 2008),
248 is described in more detail in the paper by Parhizkar et al. (2020a). To summarise, the
249 samples were extracted from the soil using a steel ring (diameter of 0.1 m and height of
250 0.05 m), after removing rocks, weeds, and litter from the soil surface. Then the soil cores in

251 the ring were transported to the laboratory, with the maximum care, to avoid soil
252 disturbance.

253

254 2.3. Soil analyses

255

256 An additional set of 100 soil samples (25 samples \times 4 tree species) was randomly collected
257 in the same locations, to measure the root system biomass (RSB, by the washing method
258 over a 1-mm sieve and subsequent oven drying at 65 °C), soil content of organic matter
259 (OM, by the potassium dichromate colorimetric method), aggregate stability in water of soil
260 (AS, De Leenheer and De Boodt, 1959), and bulk density (BD) (both using the wet-sieving
261 and oven-drying methods).

262

263 2.4. Measurement of rill detachment capacity

264

265 A laboratory-scale flume with a rectangular cross section (length of 0.5 m and width of 0.2
266 m) was used to generate rill flow to evaluate the rill detachment capacity (D_c , [$\text{kg s}^{-1} \text{m}^{-2}$])
267 of soil samples for each tree species at different values of flow rate and soil slope. Each
268 “experiment” was a combination of flow rate, slope gradient, and species simulated in the
269 flume, of which a complete description is reported in Asadi et al. (2011), Raei et al. (2015),
270 and Parhizkar et al. (2020a).

271 To summarise, each soil core was collected using a steel ring (Section 2.2) and inserted in a
272 hole of the flume bed, close to the downstream outlet, with the sample’s upper surface
273 adjusted to the same level as that of the flume bed surface. Then the flow rate and flume
274 profile slope were adjusted to the desired values. Using clean water fed upstream of the
275 flume, D_c and the hydraulic parameters of the water flow (Section 2.6) were measured over
276 a 5–300 second period. The experimental test ended when the depth of the eroded soil in
277 the steel ring reached 0.015 m. After each test, the sample of wet soil was oven dried at 105
278 °C for 24 h to determine its dry weight.

279 After the start of each experiment in the flume, we expected that the flow would become
280 steady. Then, using a level probe (accuracy of 1 mm), the water depth (h , [m]) was
281 measured at three points (0.01 m from the right and left sides and in the middle for each of
282 two cross sections, located at 0.4 m and 1 m from the flume outlet). Then the mean flow
283 depth was calculated as the average value of these six measurements.

284 D_c was calculated as the average value of four replicates using equation (1):

285

$$286 \quad D_c = \frac{\Delta M}{A \cdot \Delta t} \quad (1)$$

287

288 where:

289 - ΔM [kg] = dry weight of detached soil

290 - Δt [s] = experiment duration [s]

291 - A [m²] = area of soil sample.

292

293 2.5. Experimental design

294

295 For each soil sample of the four plant species (*C. betulus*, *Q. castaneifolia*, *P. taeda*, and *P.*
296 *persica*), five water flow rates per unit width (q , 0.26, 0.35, 0.45, 0.56, and 0.67 L m⁻¹ s⁻¹)
297 and five slope gradients (S , 1%, 2%, 3%, 4%, and 5%) were simulated in the flume, and
298 each experiment consisted of four replicates. Overall, 400 soil samples (4 plant species \times 5
299 water flow rates \times 5 slope gradients \times 4 replications) were subjected to the experiments.

300

301 2.6. Determination of the hydraulic parameters

302

303 The values of q were measured five times per experiment (collecting the water into a
304 graduated plastic cylinder), while the water velocity (v , [m s⁻¹]) was estimated using the
305 fluorescent dye technique in ten replicated measurements. Water viscosity was computed
306 from the temperature. The mean velocity (V , [m s⁻¹]) was calculated reducing v by 0.6, 0.7,
307 or 0.8, when the flow was laminar, transitional or turbulent, respectively (Abrahams et al.,
308 1985).

309 In accordance with several authors (Nearing et al., 1997), R , Re , τ (Foster, 1982), Ω
310 (Bagnold, 1966), and ω (Yang et al., 1972) were calculated using the following equations:

311

$$312 \quad R = \frac{h \cdot p}{2p + h} \quad (2)$$

313

$$314 \quad \tau = \rho g R S \quad (3)$$

315

$$316 \quad \Omega = \rho g S q \quad (4)$$

317

318 and

319

$$320 \quad \omega = SV \quad (5)$$

321

322 where:

323 - g = gravity acceleration [m s^{-2}]

324 - p = flume width [m]

325 - R = hydraulic radius [m]

326 - Re = Reynolds number [-]

327 - α = kinetic energy correction (in this case assumed as one)

328 - ρ = water density [kg m^{-3}]

329 - ω = unit stream power [m s^{-1}]

330 - Ω = stream power [kg s^{-3}].

331

332 The values of the hydraulic parameters calculated for each flow rate and profile slope in the
333 experimental flume are reported in Table 2(SD) of the Supplementary Data.

334

335 *2.7. Modelling of rill detachment capacity and rill erodibility*

336

337 The measured values of D_c (considered as the dependent variable) were regressed on ω
338 (independent variable) using linear and non-linear equations (the latter with power or
339 logarithmic functions) for each tree species, to identify the most accurate predictive model.

340 The accuracy of these equations was checked using a set of statistics (mean, standard
341 deviation, minimum and maximum values), and summary and difference indexes: the
342 coefficient of determination (R^2), coefficient of efficiency (E), root mean square error
343 (RMSE), and coefficient of residual mass (CRM). The equations to calculate these indexes
344 with the acceptance limits are reported in Table 2 (Zema et al., 2012; Krause et al., 2005;
345 Moriasi et al., 2007; Van Liew and Garbrecht, 2003).

346

347 Table 2 - Indexes and related equations, and range of variability to evaluate the prediction
 348 capacity of the models.

349

Index	Equation	Range of variability	Acceptance limit and notes
Coefficient of determination (R^2)	$r^2 = \left[\frac{\sum_{i=1}^n (O_i - \bar{O})(P_i - \bar{P})}{\sqrt{\sum_{i=1}^n (O_i - \bar{O})^2} \sqrt{\sum_{i=1}^n (P_i - \bar{P})^2}} \right]^2$	0 to 1	> 0.5 (Santhi et al., 2001; Van Liew et al., 2003; Vieira et al., 2018)
Coefficient of efficiency (E, Nash and Sutcliffe, 1970)	$E = 1 - \frac{\sum_{i=1}^n (O_i - P_i)^2}{\sum_{i=1}^n (O_i - \bar{O})^2}$	$-\infty$ to 1	“Good” model accuracy if $E \geq 0.75$, “satisfactory” if $0.36 \leq E < 0.75$ and “unsatisfactory” if $E < 0.36$ (Van Liew and Garbrecht, 2003)
Root mean square error (RMSE)	$RMSE = \sqrt{\frac{\sum_{i=1}^n (P_i - O_i)^2}{n}}$	0 to ∞	< 0.5 of observed standard deviation (Singh et al., 2004)
Coefficient of residual mass (CRM or PBIAS, Loague and Green, 1991)	$CRM = \frac{\sum_{i=1}^n O_i - \sum_{i=1}^n P_i}{\sum_{i=1}^n O_i}$	$-\infty$ to ∞	< 0.25 (Moriasi et al., 2007) - CRM < 0 indicates model underestimation - CRM > 0 indicates model overestimation (Gupta et al., 1999)

350 Notes: n = number of observations; O_i , P_i = observed and predicted values at the time step i; \bar{O} = mean of
 351 observed values.

352

353 Finally, the rill erodibility (K_r , [$s \text{ m}^{-1}$]) was estimated as the slope and intercept of equation
 354 (6) (Nearing et al., 1989):

355

356
$$D_C = K_r(\tau - \tau_c) \tag{6}$$

357

358 where:

359 - τ = hydraulic shear stress [Pa]

360 - τ_c = critical shear stress [Pa]

361

362

363 2.8. Statistical analysis

364

365 The statistical significance ($p < 0.05$) of the differences in the soil properties among the tree
366 species was evaluated using the *t*-test. The samples were assumed to be independent, and
367 their distribution was checked by QQ-plots.

368 Then, the analysis of covariance (ANCOVA) was applied to D_c (dependent variable), using
369 the tree species (categorical variable), and the slope and flow rate (numerical variables) as
370 factors. The pairwise comparison by Tukey's test (at $p < 0.05$) was also used to evaluate the
371 statistical significance of the differences in D_c among the tree species. To satisfy the
372 assumptions of the statistical tests (equality of variance and normal distribution of
373 samples), the data were subjected to a normality test or were square root-transformed
374 whenever necessary.

375 Finally, Pearson's matrix was calculated to find correlations among the soil properties. The
376 principal component analysis (PCA) was also applied to the soil properties to select a few
377 derivative parameters and to cluster soil samples in groups related to each tree species.

378 All statistical analyses were conducted by XLSTAT 9.0 software (Addinsoft, Paris,
379 France).

380

381 3. Results

382

383 3.1. Variability of soil properties and rill detachment capacity among the tree species

384

385 The texture of the soil samples was silty clay loam (according to the USDA classification,
386 33% clay, 46% silt, and 19% sand), without significant variations among the tree species.
387 The differences in texture and bulk density (on average 1359 kg m^{-3}) of the soil samples
388 were not significant (Table 3). Conversely, the other soil properties were in general
389 significantly different among the tree species. More specifically, the aggregate stability was
390 higher (0.72 ± 0.05) in *P. persica* and lower (0.48 ± 0.06) in *C. betulus*. The latter species
391 showed the lowest root system biomass ($0.51 \pm 0.03 \text{ kg m}^{-3}$), while the maximum value

392 ($0.87 \pm 0.02 \text{ kg m}^{-3}$) was recorded in *C. betulus* Organic matter was $1.63 \pm 0.01\%$ in *C.*
 393 *betulus*, $1.73 \pm 0.01\%$ in *Q. castaneifolia*, $1.96 \pm 0.01\%$ in *P. persica*, and 1.84 ± 0.02 in *P.*
 394 *taeda* The differences in OM content among the species were significant, except for *C.*
 395 *betulus* and *Q. castaneifolia* (Table 1).

396

397 Table 3 - Main properties (mean \pm standard deviation) of forest soil sampled under four
 398 tree species in Saravan Forest Park (Northern Iran).

399

Soil property		Tree species			
		<i>C. betulus</i>	<i>Q. castaneifolia</i>	<i>P. persica</i>	<i>P. taeda</i>
Texture (%)	ClC	$33.8 \pm 0.33 \text{ a}$	$33.7 \pm 0.46 \text{ a}$	$33.5 \pm 0.24 \text{ a}$	$33.5 \pm 0.23 \text{ a}$
	SiC	$46.9 \pm 0.61 \text{ a}$	$46.8 \pm 0.60 \text{ a}$	$46.7 \pm 0.35 \text{ a}$	$46.9 \pm 0.35 \text{ a}$
	SaC	$19.3 \pm 0.47 \text{ a}$	$19.5 \pm 0.25 \text{ a}$	$19.8 \pm 0.25 \text{ a}$	$19.6 \pm 0.23 \text{ a}$
<i>BD (kg m⁻³)</i>		$1384 \pm 12.29 \text{ a}$	$1366 \pm 10.50 \text{ a}$	$1331 \pm 13.99 \text{ a}$	$1355 \pm 11.73 \text{ a}$
<i>RSB (kg m⁻³)</i>		$0.51 \pm 0.03 \text{ a}$	$0.62 \pm 0.02 \text{ b}$	$0.87 \pm 0.02 \text{ c}$	$0.70 \pm 0.07 \text{ b}$
<i>AS (-)</i>		$0.48 \pm 0.06 \text{ a}$	$0.55 \pm 0.04 \text{ a}$	$0.72 \pm 0.05 \text{ b}$	$0.61 \pm 0.06 \text{ c}$
<i>OM (%)</i>		$1.63 \pm 0.01 \text{ a}$	$1.73 \pm 0.01 \text{ a}$	$1.96 \pm 0.01 \text{ b}$	$1.84 \pm 0.02 \text{ c}$

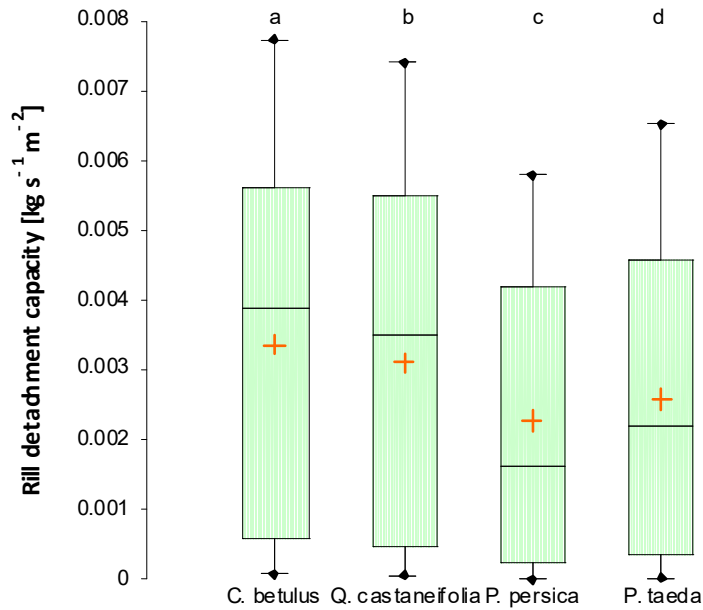
400 Notes: OM = organic matter content; BD = bulk density; RSB = root system biomass; AS = aggregate
 401 stability; SaC = sand content; SiC = silt content; ClC = clay content; the letters indicate significant differences
 402 among tree species at $p < 0.05$ of the *t*-test ($n = 25$ for each species).

403

404 D_c was significantly influenced by the tree species ($p < 0.05$). The mean value was the
 405 highest for *C. betulus* ($0.00336 \text{ kg m}^{-2} \text{ s}^{-1}$) and the lowest for *P. persica* ($0.00226 \text{ kg m}^{-2}$
 406 s^{-1}). Therefore, the ratio between the maximum and minimum D_c was on average 1.49. *Q.*
 407 *castaneifolia* and *P. taeda* had intermediate D_c (0.0031 and $0.0026 \text{ kg m}^{-2} \text{ s}^{-1}$, respectively)
 408 between the extreme values. The variability of D_c is noticeable among the tree species, as
 409 shown by coefficients of variation (ratio of standard deviation by mean) between 78.4% (*C.*
 410 *betulus*) and 92.9% (*P. persica*) (Figure 3).

411

412



Different letters indicate significant differences after ANOVA at $p < 0.05$.

413
414
415

416 Figure 3 - Box-whisker plot of rill detachment capacity in forest soils sampled under four
417 tree species in Saravan Forest Park (Northern Iran) ($n = 25$ for each species).
418

419 Pearson's matrix shows that the correlations of D_c with the other soil properties were
420 generally low (coefficient of correlation $R < 0.27$) and significant only with the root system
421 biomass ($R = -0.257$) and aggregate stability ($R = -0.261$). Conversely, the correlations
422 between the other pairs of soil properties were high and significant. For instance, the
423 organic matter content was correlated with the root system biomass ($R = 0.942$), aggregate
424 stability ($R = 0.837$), and bulk density ($R = -0.843$). Moreover, the correlations among the
425 latter soil properties were also high ($R = -0.789$ between the bulk density and the root
426 system biomass, -0.686 between the bulk density and the aggregate stability, and 0.840
427 between the root system biomass and the aggregate stability). As regards the soil texture,
428 only the silt content was significantly correlated with sand ($R = -0.507$) and clay ($R = -$
429 0.470), although R was not high (Table 4).

430

431 Table 4 - Pearson's correlation matrix among the properties of forest soils sampled under
432 four tree species ($n = 25$ for each species) in Saravan Forest Park (Northern Iran).
433

Soil property	D_c	OM	BD	RSB	AS	SaC	SiC	ClC
D_c		-0.159	-0.045	-0.257	-0.261	-0.057	0.097	0.083

OM			-0.843	0.942	0.837	0.230	-0.289	-0.141
BD				-0.789	-0.686	-0.237	0.240	0.174
RSB					0.840	0.220	-0.243	-0.143
AS						0.135	-0.222	-0.079
SaC							-0.507	0.059
SiC								-0.470
CIC								

434 Notes: D_c = rill detachment capacity; OM = organic matter content; BD = bulk density; RSB = root system
435 biomass; AS = aggregate stability; SaC = sand content; SiC = silt content; CIC = clay content; values in bold
436 are different from 0 at p level < 0.01.

437

438 PCA provided three principal components (PCs), which explained 48.7% (PC_1), 24.7%
439 (PC_2), and 13.0% (PC_3) of the total variance of the properties of the soils collected under
440 the four tree species. The first two PCs explained 73.3% of this variance. The properties
441 related to the soil texture had significant loadings on PC_2 (very high for clay, over 0.90).
442 The other soil properties significantly influenced the first PC with high loadings (over
443 0.75), while D_c heavily weighed on PC_3 (loading of 0.92) (Table 5). In other words, these
444 loadings confirm the results of Pearson's correlations (high r coefficients and therefore
445 strong associations among organic matter, bulk density, root system biomass, and aggregate
446 stability), but no direct association was found between D_c and the other soil properties
447 (Table 5 and Figure 4a).

448

449

450 Table 5 - Loadings of the original variables (properties of forest soils collected under four
451 tree species) on the first two principal components (PC_1 and PC_2) ($n = 25$ for each species
452 in Saravan Forest Park, Northern Iran).

453

Soil properties	Principal components		
	PC_1	PC_2	PC_3
D_c	0.053	0.000	0.921
OM	0.928	0.010	0.003
BD	0.754	0.002	0.091
RSB	0.901	0.011	0.004
AS	0.782	0.008	0.013

SaC	0.342	0.332	0.005
SiC	0.050	0.945	0.000
ClC	0.083	0.665	0.005

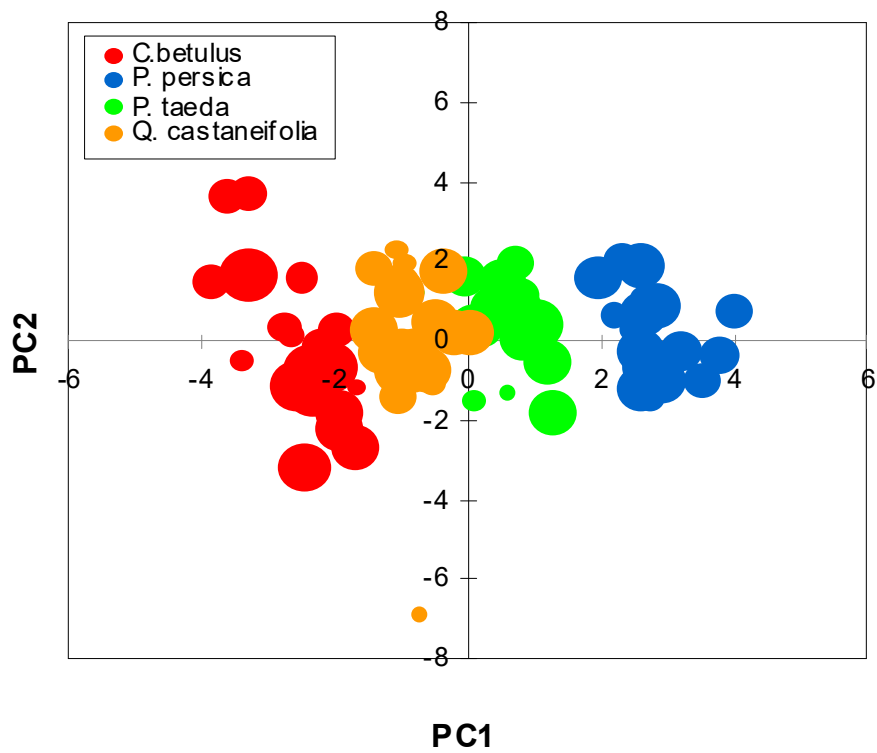
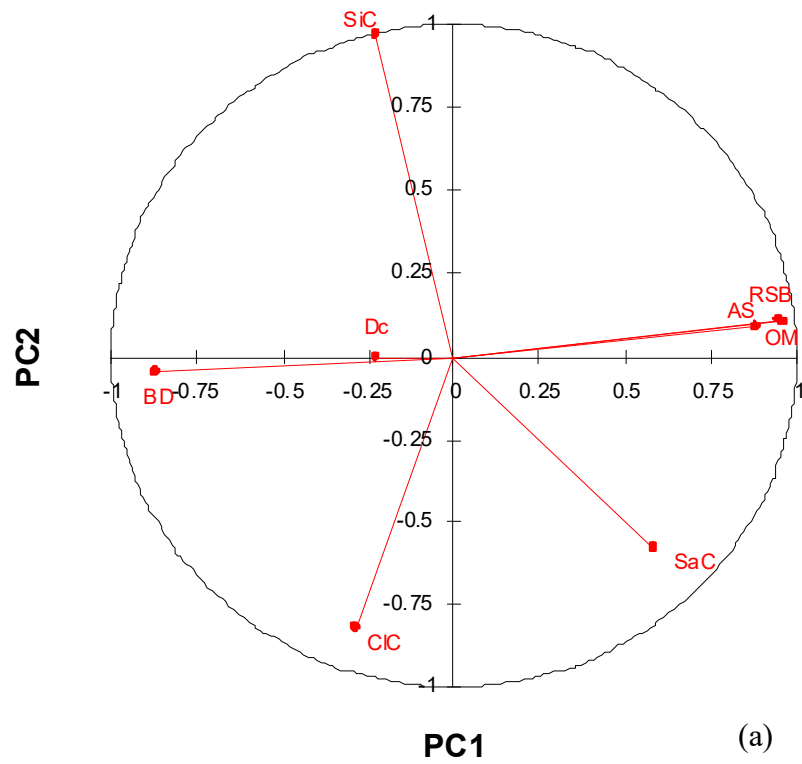
454 Notes: D_c = rill detachment capacity; OM = organic matter content; BD = bulk density; RSB = root system
455 biomass; AS = aggregate stability; SaC = sand content; SiC = silt content; ClC = clay content; values in bold
456 correspond for each variable to the factor for which the loading is the largest.

457

458 The plot of the sample scores on the first three PCs shows clear differences in soil properties among the
459 studied tree species. Four well-differentiated groups, one for each tree species, are
460 evidenced, with only a limited overlapping of groups for the *P. taeda* and *Q. castaneifolia*
461 species (Figure 4b).

462

463



464

465 Legend: D_c = rill detachment capacity; OM = organic matter content; BD = bulk density; RWD = root system

466 biomass; AS = aggregate stability; SaC = sand content; SiC = silt content; CIC = clay content; PC = principal

467

component.

468

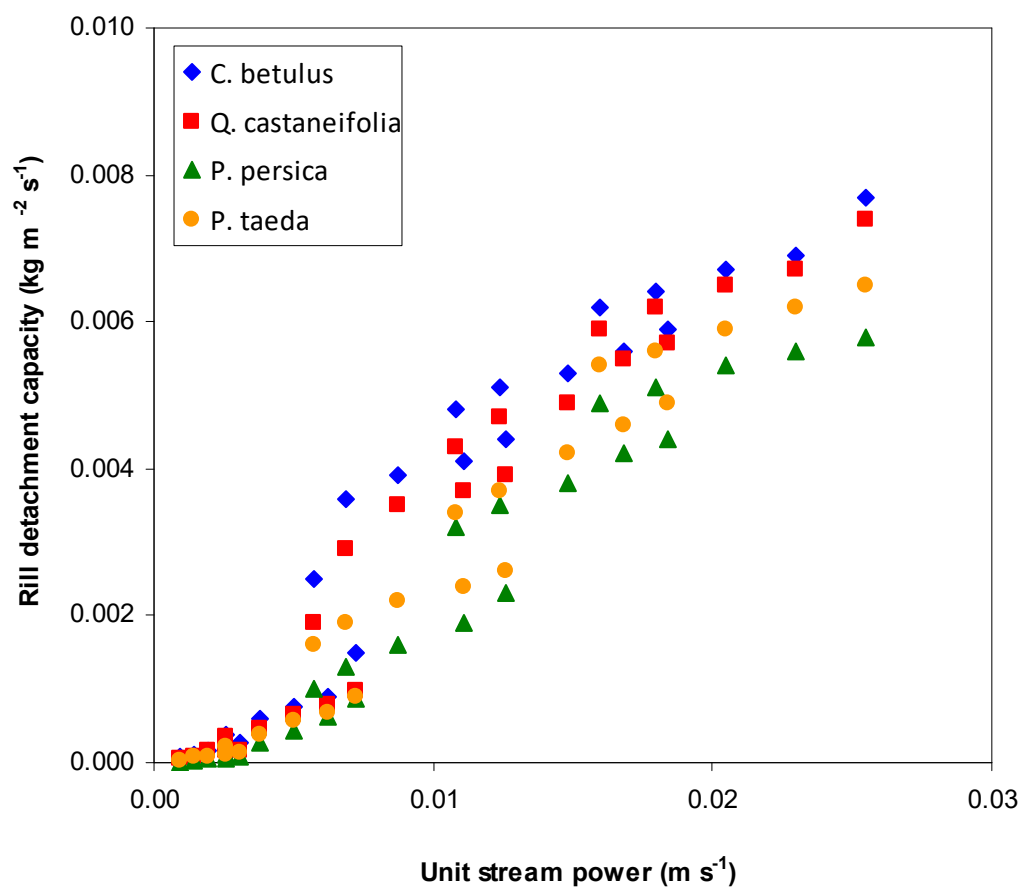
469 Figure 4 - Loadings of soil parameters (a), and scores of forest soil samples (b) on the first
470 two principal components (PC) for four tree species in Saravan Forest Park (Northern
471 Iran). (The circle size is proportional to the values of the third PC.)

472

473 3.2. Relationships among rill detachment capacity and unit stream power and estimation of
474 rill erodibility

475

476 Figure 5 shows that at low values of the unit stream power ω ($< 0.005\text{--}0.006 \text{ m s}^{-1}$) the
477 differences in D_c were small; moreover, these differences increased with ω .



478

479 Figure 5 - Correlations between the rill detachment capacity and unit stream power in forest
480 soils sampled under four tree species in Saravan Forest Park (Northern Iran) ($n = 25$ for
481 each species).

482

483 In the previous study by Parhizkar et al. (2020a), the best predictor of D_c in forests was ω ,
484 and the interpolating equation was a power function. In this investigation, when the two
485 variables were regressed using power equations, the coefficients of determination were high
486 ($R^2 > 0.85$), but the prediction capacity of these equations (different for each tree species)

487 was not always good, as shown by the values of E (> 0.75 only for *P. taeda*) (Tables 6 and
 488 7). Adopting a linear equation, the values of R^2 and E increased for three of the four tree
 489 species. Only one model (for *P. persica*) was not accurate (E = 0.43), due to the large
 490 overestimation of D_c . The best model to predict D_c from ω was a logarithmic equation, for
 491 which all the evaluation indexes were good and the statistics (e.g., mean and maximum
 492 values) between predictions and observations were very close. However, in some cases
 493 (that is, at very low ω) the model gives negative values of D_c , and this suggests application
 494 only in the case of $\omega > 0.0025 \text{ m s}^{-1}$. This limitation is acceptable, because a low ω
 495 characterizes water flow with limited erosive power. In general, all the equations
 496 overestimated the observed D_c , as shown by the negative CRM, but the RMSE was always
 497 satisfactory (except for the linear equation applied to *P. persica*) (Tables 6 and 7).

498

499 Table 6 - The equations correlating D_c ($\text{kg m}^{-2} \text{ s}^{-1}$) with the unit stream power (ω , m s^{-1}) in
 500 forest soils sampled under four tree species in Saravan Forest Park (Northern Iran) ($n = 25$
 501 for each species).

502

Function	Tree species	Equation
Power	<i>C. betulus</i>	$D_c = 3.620 \omega^{1.559}$
	<i>Q. castaneifolia</i>	$D_c = 4.673 \omega^{1.640}$
	<i>P. persica</i>	$D_c = 17.744 \omega^{2.024}$
	<i>P. taeda</i>	$D_c = 5.434 \omega^{1.720}$
Linear	<i>C. betulus</i>	$D_c = 0.3487 \omega + 0.0002$
	<i>Q. castaneifolia</i>	$D_c = 0.3420 \omega + 0.0004$
	<i>P. persica</i>	$D_c = 0.3061 \omega + 0.0006$
	<i>P. taeda</i>	$D_c = 0.2820 \omega + 0.0006$
Logarithmic	<i>C. betulus</i>	$D_c = 0.0026 \ln \omega + 0.0163$
	<i>Q. castaneifolia</i>	$D_c = 0.0025 \ln \omega + 0.0156$
	<i>P. persica</i>	$D_c = 0.0020 \ln \omega + 0.1220$
	<i>P. taeda</i>	$D_c = 0.0022 \ln \omega + 0.0134$

503 Table 7 - Values of the criteria adopted for evaluating the accuracy of equations in Table 6 to predict the rill detachment capacity from the unit
 504 stream power in soils sampled under four tree species in Saravan Forest Park (Northern Iran).
 505

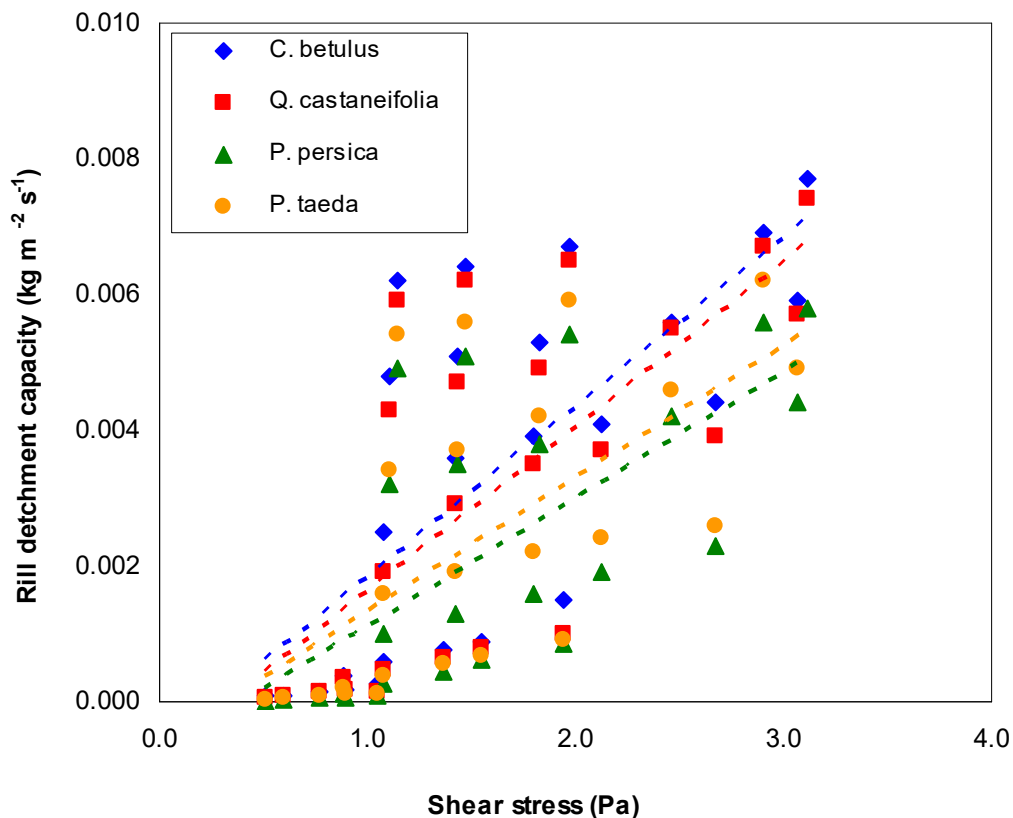
Equation structure	Tree species	Soil detachment capacity	Statistic				Index			
			Mean	Minimum	Maximum	Standard deviation	R ²	E	CRM	RMSE
Power	<i>C. betulus</i>	<i>Observed</i>	0.0034	0.0001	0.0077	0.0026	0.85	0.71	-0.03	0.001
		<i>Predicted</i>	0.0035	0.0001	0.0119	0.0034				
	<i>Q. castaneifolia</i>	<i>Observed</i>	0.0031	0.0001	0.0074	0.0026	0.85	0.71	-0.03	0.001
		<i>Predicted</i>	0.0032	0.0000	0.0114	0.0032				
	<i>P. persica</i>	<i>Observed</i>	0.0023	0.0000	0.0058	0.0021	0.86	0.63	-0.11	0.001
		<i>Predicted</i>	0.0025	0.0000	0.0106	0.0029				
	<i>P. taeda</i>	<i>Observed</i>	0.0026	0.0000	0.0065	0.0023	0.90	0.82	-0.04	0.001
		<i>Predicted</i>	0.0027	0.0000	0.0099	0.0028				
Linear	<i>C. betulus</i>	<i>Observed</i>	0.0034	0.0001	0.0077	0.0026	0.92	0.90	-0.12	0.001
		<i>Predicted</i>	0.0038	0.0005	0.0091	0.0025				
	<i>Q. castaneifolia</i>	<i>Observed</i>	0.0031	0.0001	0.0074	0.0026	0.94	0.84	-0.26	0.001
		<i>Predicted</i>	0.0039	0.0007	0.0091	0.0025				
	<i>P. persica</i>	<i>Observed</i>	0.0023	0.0000	0.0058	0.0021	0.95	0.43	-0.65	0.002
		<i>Predicted</i>	0.0037	0.0009	0.0084	0.0022				

	<i>P. taeda</i>	<i>Observed</i>	0.0026	0.0000	0.0065	0.0023	0.96	0.78	-0.36	0.001
		<i>Predicted</i>	0.0035	0.0009	0.0078	0.0020				
<i>Logarithmic</i>	<i>C. betulus</i>	<i>Observed</i>	0.0034	0.0001	0.0077	0.0026	0.87	0.86	-0.05	0.001
		<i>Predicted</i>	0.0035	-0.0019	0.0068	0.0024				
	<i>Q. castaneifolia</i>	<i>Observed</i>	0.0031	0.0001	0.0074	0.0026	0.85	0.84	-0.07	0.001
		<i>Predicted</i>	0.0033	-0.0019	0.0064	0.0023				
	<i>P. persica</i>	<i>Observed</i>	0.0023	0.0000	0.0058	0.0021	0.80	0.80	-0.05	0.001
		<i>Predicted</i>	0.0024	-0.0018	0.0049	0.0019				
	<i>P. taeda</i>	<i>Observed</i>	0.0026	0.0000	0.0065	0.0023	0.90	0.82	-0.04	0.001
		<i>Predicted</i>	0.0027	0.0000	0.0099	0.0028				

506

Notes: R^2 = coefficient of determination; E = coefficient of efficiency of Nash and Sutcliffe; RMSE = Root Mean Square Error; CRM = Coefficient of Residual Mass.

507 When D_c was regressed on the shear stress τ using equation (6), the slope (the rill
 508 erodibility K_r) and intercepts (the critical shear stress τ_c) of soils were different among the
 509 tree species. These equations had coefficients of regression (R^2) between 0.48 and 0.52,
 510 always significant at $p < 0.05$ (Table 8 and Figure 5). The soils with *C. betulus* and *P.*
 511 *persica* showed the maximum (0.0025 s m^{-1}) and minimum (0.0019 s m^{-1}) values of K_r ,
 512 respectively, corresponding to the minimum (0.28 Pa) and maximum (0.42 Pa) values of τ_c .
 513 K_r of the soil with *C. betulus* soil was 1.04, 1.19, and 1.31 times greater than *Q.*
 514 *castaneifolia*, *P. taeda*, and *P. persica* soils, while τ_c of soils under *P. persica* was 1.5, 1.3,
 515 and 1.1 times the values of *C. betulus*, *Q. castaneifolia*, and *P. taeda*, respectively (Table
 516 8).
 517



518
 519 Figure 6 - Linear regression equations between the rill detachment capacity and the shear
 520 stress to estimate the rill erodibility and the critical shear stress in forest soils sampled
 521 under four tree species in Saravan Forest Park (Northern Iran) ($n = 25$ for each species).
 522

523 Table 8 - Results of regression analysis between the rill detachment capacity (D_c) and the
 524 shear stress (τ) to estimate the rill erodibility (K_r) and the critical shear stress (τ_c) in forest

525 soils sampled under four tree species in Saravan Forest Park (Northern Iran) ($n = 25$ for
526 each species).

527

Tree species	Linear regression equation (6)	K_r (s m^{-1})	τ_c (Pa)	R^2
<i>C. betulus</i>	$D_c = 0.0025 \tau - 0.0007$	0.0025	0.28	0.52
<i>Q. castaneifolia</i>	$D_c = 0.0024 \tau - 0.0008$	0.0024	0.33	0.52
<i>P. persica</i>	$D_c = 0.0019 \tau + 0.0008$	0.0019	0.42	0.47
<i>P. taeda</i>	$D_c = 0.0021 \tau - 0.0008$	0.0021	0.38	0.48

528

Note: R^2 = coefficient of determination.

529

530 4. Discussions

531

532 4.1. Effects of the tree species on soil properties and rill detachment capacity

533

534 The present study has explored whether four dominant tree species are able to induce
535 changes in the erodibility of forest soils with homogenous texture (silty clay loam class)
536 and similar properties (which are presumably due to the same forming processes and
537 similar parent materials, Foth et al., 1990). Given this soil homogeneity, the plant survival
538 and growth dynamics of the four tree species, combined with some practices used in this
539 forest (such as forest improvement, timber harvesting, prescribed burning, and thinning),
540 may explain the surveyed variations in the soil properties and rill detachment capacity.

541 The higher bulk density values and the lower aggregate stability of the soil with *C. betulus*
542 could be due to the root system characteristics of this species. *C. betulus* has few surface
543 roots (low weight density), which are responsible for a decrease in organic matter, strongly
544 linked to the properties mentioned above. This is also confirmed by the correlation analysis,
545 showing that, when the organic matter of soil increased, root system biomass and aggregate
546 stability also increased. Conversely, soils with *P. persica*, which have a considerable
547 surface roughness and structure (Viles et al., 1990; Gyssels et al., 2005), showed a higher
548 root system biomass, organic matter content, and aggregate stability. Moreover, in these
549 soils the bulk density was found to be lower, because the roots contribute to create a system
550 of continuous pores (Gyssels et al., 2005, Angers and Caron, 1998; Shinohara et al., 2016).
551 This result is in accordance with Shinohara et al. (2016) and David (2000), who showed
552 that soil bulk density decreases with the presence of plant roots. Also Li et al. (1992; 1993)

553 reported that fine roots less than one mm in diameter can significantly decrease the bulk
554 density of soil and increase soil porosity). Furthermore, soil bulk density mainly depends
555 on root diameter. As found by Meek et al. (1992), an increase in fine roots (less than one
556 mm) implies a decrease in bulk density, while larger roots work in the opposite direction,
557 which is consistent with several studies (e.g., Gyssels et al., 2005; Mamo and Bubenzer,
558 2001a; 2001b). In general, it has been demonstrated that species with high root density have
559 the highest potential to reduce soil erosion rates by concentrated flow (De Baets et al.,
560 2007).

561 The variability of the soil properties between the tree species having different root
562 characteristics confirms that plant roots play a key role in driving changes in the soil. This
563 leads to the conclusion that root density and structure, which vary among plant species, also
564 exert an influence on soil detachment (Wang et al., 2015; Zhang et al., 2013; Li et al.,
565 2015). In general, it has been demonstrated that rill erodibility and soil detachment rates
566 decreased exponentially with root density (De Baets et al., 2007). More specifically, Wang
567 et al. (2018b) found that soil detachment capacity decreases exponentially with root system
568 biomass among two different types of root systems in grasslands. Li et al. (1991a) have
569 demonstrated that soils with *Pinus tabulaeformis* (a conifer) and *Hippophae rhamnoides* (a
570 typical tree and shrub in the Chinese Loess Plateau) show an exponentially decreasing trend
571 of soil detachment by rills with root density. Also Gyssels and Poesen (2003) indicated that
572 rill erosion decreases exponentially with increasing root densities of cereals and grasses in
573 the loess Belt of Central Belgium, which is probably due to the combined effect of roots
574 and shoots of vegetation on soil erosion. This influence results in noticeable changes in rill
575 detachment capacity, which in this study varied significantly among the four tree species.
576 The lowest root system biomass detected in soils with *C. betulus* explains the minor effect
577 of this species on soil resistance to rill erosion. Additionally, exposing the soil with *C.*
578 *betulus* to some management operations (e.g., prescribed burning, thinning) may have
579 contributed to reducing the rill detachment capacity of this soil.

580 The lowest value of rill detachment capacity measured in soils with *P. persica* may be due
581 to the highest root system biomass, and this is consistent with the results of other studies
582 (Bibalani et al., 2006; Abdi et al., 2010). The latter authors found that the characteristics of
583 the root system of *P. persica* enhance the stability of slopes by increasing the shear
584 resistance of the soil, and this usually helps to minimize the risk of shallow landslides.
585 Other studies (Wang et al., 2015; Li et al., 1991a; Li, 1995) have also concluded that plant
586 roots are very important in reducing soil detachment, and specifically rill erosion (De Baets

587 et al., 2005; Gyssels et al., 2005). The study by Wang et al. (2015) stated that plant roots
588 have the greatest effect on increasing soil resistance to erosion, compared with other
589 contributory factors. However, other investigations have shown that vegetation cover might
590 not be so important or is even insignificant for controlling rill erosion (De Baets et al.,
591 2007; Wang et al., 2014a). The fine and fibrous roots of *P. persica* increase soil stability
592 and decrease its susceptibility to water erosion compared to the soils under other tree
593 species. Moreover, root system biomass is commonly used to explain the influence of plant
594 roots on soil detachment capacity. In this study, the highest root system biomass played
595 more pronounced effects on the rill detachment capacity of soils with *P. persica* compared
596 to the soils from the other tree species. The present study and the related literature indicate
597 therefore that, for reducing rill erosion rates in erosion-sensitive areas (such as semi-arid
598 forests) it is recommended to use plant species that develop a dense root network (i.e., with
599 fibrous roots, De Baets et al., 2007). Moreover, management actions targeted at soil
600 stabilization should be prioritized in these forest ecosystems, and deforestation, especially
601 in *P. persica* areas, should be avoided to control soil erosion.

602 The correlation analysis and PCA confirmed the relationships between the most important
603 properties and erodibility of the experimental soils. These statistical techniques
604 demonstrated that, for the investigated tree species in forests, the rill detachment capacity
605 was directly associated with the root system biomass and aggregate stability of sampled
606 soils. This result is in accordance with Li et al. (1992a), who found that plant roots
607 significantly increase soil's structural stability, and thus decrease its erodibility. In other
608 words, when root system biomass and aggregate stability decrease, rill detachment capacity
609 increases.

610 Moreover, the three principal components provided by PCA individually synthesized the
611 physical properties, the textural characteristics and the rill detachment capacity of soils. The
612 clustering of soils in four groups (one for each tree species) showed a clear gradient
613 according to the physical properties of the soil. Also in the studies of Lucas-Borja et al.
614 (2020) and Shabanpour et al. (2020) - the latter carried out in the same environment - the
615 differences in soil properties among different land uses (abandoned farmland, intensive
616 cropland, grassland, forestland, and woodland) were evident, and well-differentiated
617 groups, one for each land use, were clustered. In this study, these differences went beyond
618 land uses (therefore the landscape scale) and down to a smaller spatial scale; this means that
619 rill detachment capacity is different not only among different land uses (as several studies
620 have demonstrated, e.g., Parhizkar et al., 202a; Shabanspour et al., 2020), but also among

621 soils with a specific but dominant tree species, since the latter induces significant
622 variations in soil's physical properties due to the action of its root system. This means that
623 changes in soil properties, due to an individual tree species with its specific root actions, are
624 important drivers of soil detachability in forests. A large body of literature shows that roots
625 affect soil properties - such as infiltration rates, aggregate stability, water and organic
626 matter contents, and shear strength - all controlling soil erosion rates to various degrees, not
627 only in forests but in the majority of land uses (e.g., De Baets et al., 2007; Vogt et al., 1995;
628 Lu et al., 2020).

629 In addition to the effects of tree root systems, soil erosion (and, therefore, the detachment
630 component of this complex physical process) are influenced by other ecological
631 characteristics of forest plants that drive soil hydrology. For instance, trees are also
632 important in forest hydrology because of the interception of rainfall by their canopies,
633 which reduces beneath-canopy throughfall and, ultimately, runoff and soil loss (Yang et al.,
634 2019). In this regard, *P. persica*, *C. betulus* and *Q. castaneifolia*, although deciduous, have
635 broad leaves that are arranged on the branches with a wide canopy, which increases
636 interception (Nasiri et al., 2012). Conversely, the needles of *P. taeda* have a lower surface
637 area that is not so effective at reducing canopy throughfall, but they do protect soil from the
638 kinetic energy of intense storms, even in the wettest seasons. Moreover, the aboveground
639 biomass of tree species can also reduce the hydrological response of soils, increasing
640 hydraulic roughness and trapping sediments (Kervroëdan et al., 2018). All these
641 characteristics of trees must be taken into account in addition to their root system features,
642 when specific tree species have to be selected for erosion control.

643

644 4.2. Relationships between rill detachment capacity, rill erodibility, and unit stream power

645

646 Beside root characteristics and other hydrological factors linked to individual tree species,
647 rill detachment capacity depends on the hydraulic characteristics of overland flow (Nearing
648 et al., 1991). The regression analysis carried out in this study confirmed that unit stream
649 power is a good predictor of rill detachment capacity. This high accuracy may be due to the
650 fact that unit stream power simultaneously takes into account the flow velocity and soil
651 slope, both influencing soil detachability due to overland flow (Parhizkar et al., 2020a).
652 These results are in accordance with several studies, showing that rill detachment capacity
653 by overland flow was closely related to flow characteristics, such as water discharge, shear
654 stress, stream power, unit stream power, and unit energy; thus, rill detachment capacity can

655 be estimated from one of these predictors (Nearing et al., 1991; Xiao et al., 2017; Li et al.,
656 2019). Moreover, our results showed that, compared to the power equations identified in
657 the previous study for forests (Parhizkar et al., 2020a), a logarithmic function was more
658 accurate at estimating the rill detachment capacity from the unit stream power for the
659 different tree species. However, there is no physical reason for this higher accuracy, since
660 our method was simply based on a “black-box” approach (Nearing et al., 1991), looking for
661 the most accurate equation and the best predictor of a hydrological variable. This approach
662 is used in several environmental studies, where the combination of complex physical,
663 chemical and biological processes makes it practically impossible to create simulations on a
664 mathematical basis, apart from simple regressions with variable analytical forms. The
665 regression equations are site-specific, and must be calibrated and used in the same or a least
666 in a very similar environment. The models are very useful for those users who require an
667 order of magnitude of soil erodibility in a soil with a specific tree species.

668 The response curves of rill detachment capacity versus the hydraulic parameter chosen in
669 this study (unit stream power) showed that the coefficients of the regression equations were
670 very similar for three of the studied species (*C. betulus*, *Q. castaneifolia*, and *P. taeda*),
671 while *P. persica* had a higher intercept (that is, rill detachment capacity in the case of zero
672 stream power) and a lower slope (that is, rill detachment capacity increases less with unit
673 stream power compared to the other species). This is further proof that soil erodibility is
674 influenced not only by its physical properties, but also by the ecological features of plants,
675 such as their root systems.

676 The rill detachment capacity of a soil due to overland flow is strictly linked to its rill
677 erodibility and critical shear stress, which are two of the most important variables reflecting
678 soil resistance to rill erosion (Nearing et al., 1989). In the context of the previous
679 discussion, it is important to evaluate the effects of tree species in forests on these
680 variables, which are highly sensitive input parameters of some process-based erosion
681 models (Wang et al., 2016), such as the Water Erosion Prediction Project (WEPP) (Laflen
682 et al., 1991). The regression equations set up in this study for the four tree species went in
683 this direction, because they are the algorithm on which the erosion component of WEPP is
684 based. Since rill erosion is the prevalent form in process-based erosion models, rill
685 detachment capacity and erodibility are key parameters for accurate predictions of erosion
686 (Wang et al., 2016; Nearing et al., 1989). Therefore, their quantification is important to
687 improve the prediction accuracy of the WEPP model applications in arid areas.

688 However, the predictive accuracy of these equations, although satisfactory, was not as high
689 as the models developed by Parhizkar et al. (2020a) and Zhang et al. (2008). Both these
690 studies found that the linear regression functions between soil detachment and shear stress
691 were very high for several land uses, with coefficients of determination of up to 0.9. Our
692 study relates to a different spatial scale, and this may have influenced the lower prediction
693 accuracy of the developed equations.

694 Compared to the other tree species, *P. persica* showed the lowest rill erodibility and the
695 highest critical shear stress. This was an effect of the lowest rill detachment capacity, which
696 was due to the binding effect of roots (Wang et al., 2014a), and of the changes induced by
697 the root system on soil properties. In other words, the lower rill detachment capacity
698 detected in *P. persica* soils, which was due to the interactive effects of roots and soil
699 properties, also influenced the rill erodibility and critical shear stress, which were
700 mathematically associated with the rill detachment capacity.

701 Among the root characteristics of all the tree specie, the density and diameter of *P. persica*
702 provided the highest resistance of the soil to concentrated flow erosion. The lower rill
703 erodibility in roots with a diameter lower than one mm, known as “effective” roots (Li et
704 al., 1991b; 1992), was in accordance with previous studies, showing that these roots reduce
705 concentrated flow erosion and thus decrease the soil detachment capacity (Li et al., 1991b;
706 Li et al., 1995).

707

708 **5. Conclusions**

709

710 The soil’s physico-chemical properties (except soil texture and bulk density) and mean rill
711 detachment capacity were different among the soils with four tree species sampled in
712 Northern Iran. The soils with *Parrotia persica* and *Carpinus betulus* showed the lowest and
713 the highest rill detachment capacity, respectively. This means the research question about
714 the ability of the studied tree species with their root characteristics to reduce the rill
715 detachment capacity compared to other plants can be confirmed. The higher root system
716 biomass of *Parrotia persica* could have played a binding effect on the soil and improved its
717 aggregate stability, thanks to the higher organic matter content. Therefore, *Parrotia persica*
718 shows the highest capacity to protect soil against erosion. These results can support
719 ecological engineers in the choice of tree species that are best indicated for soil
720 conservation.

721 The most accurate equations to predict rill detachment capacity from unit stream power
722 were based on a logarithmic function for all the studied species. These equations are highly
723 accurate for water flow rates over 0.0025 m s^{-1} ; this suitability addresses the second
724 research question of this study. Rill erodibility and critical shear stress were lowest and
725 highest, respectively, in *Parrotia persica*; this confirms the higher soil protection capacity
726 against erosion of this species in comparison with the other plants. The proposed models
727 are simple but quite accurate for predicting rill detachment rates. These models are
728 particularly useful in ecological engineering applications, when the order of magnitude of
729 soil erodibility must be estimated and the most effective plant species must be selected.
730 However, further studies should be carried out to test the reliability of the suggested
731 equations in other environmental conditions.

732

733 **Acknowledgements**

734

735 This study was funded by the Spanish Ministry of Economy, Industry and Competitiveness
736 Research Projects, BIORESOC (CGL2017-88734-R). Isabel Miralles is grateful for
737 funding received from the Ramón y Cajal Research Grant (RYC-2016-21191) from the
738 Spanish Ministry of Economy, Industry and Competitiveness (MINECO).

739

740 **References**

741

742 Abdi, E., Majnounian, B., Genet, M., Rahimi, H., 2010. Quantifying the effects of root
743 reinforcement of Persian Ironwood (*Parrotia persica*) on slope stability; a case study:
744 Hillslope of Hyrcanian forests, northern Iran. *Ecological Engineering*. 36, 1409–1416.

745 Abdi, E., Deljouei, A., 2019. Seasonal and spatial variability of root reinforcement in three
746 pioneer species of the Hyrcanian forest. *Austrian Journal of Forest Science*. 136 (3), 175-
747 198.

748 Abdi, E., 2014. Effect of Oriental beech root reinforcement on slope stability (Hyrcanian
749 Forest, Iran). *Journal of forest science*. 60 (4), 166–173.

750 Abedi, R., Pourbabaei, H., 2011. Ecological species groups in the rural heritage museum of
751 Guilan Province, Iran. *Caspian J. Env. Sci*. 9 (2), 115–123.

752 Aksoy, H., Kavvas, M.L., 2005. A review of hillslope and watershed scale erosion and
753 sediment transport models. *Catena*. 64, 247–271.

754 Amoopour, M., Ghobad-nejhad, M., Khodaparast, S.A., 2016. New records of polypores
755 from Iran, with a checklist of polypores for Gilan Province. *Czech Mycology*. 68 (2), 139–
756 148.

757 An, S., Mentler, A., Mayer, H., Blum, W.E., 2010. Soil aggregation, aggregate stability,
758 organic carbon and nitrogen in different soil aggregate fractions under forestland and shrub
759 vegetation on the Loess Plateau, China. *Catena*. 81, 226–233.

760 Angers, D.A., Caron, J., 1998. Plant-induced changes in soil structure: Processes and
761 feedbacks. *Developments in Biogeochemistry*. 42, 55–72. doi:10.1023/A:1005944025343.

762 Asadi, H., Aligoli, M., Gorji, M., 2017. Dynamic changes of sediment concentration in rill
763 erosion at field experiments. *JWSS-Isfahan University of Technology*. 20(78), 125-139.

764 Asadi, H., Ghadiri, H., Rose, C.W., Yu, B., Hussein, J., 2007. An Investigation of flow-
765 driven soil erosion at low streampowers. *J. Hydrol*. 342, 134–142.

766 Asadi, H., Moussavi, A., Ghadiri, H., Rose, C.W., 2011. Flow-driven soil erosion processes
767 and the size selectivity of sediment. *J. Hydrol.*, 406, 73–81.

768 Bagnold, R.A., 1966. An approach to the sediment transport problem for general physics.
769 In U.S. Geological Survey Professional Paper 422-I; U.S. Government Printing Office:
770 Washington, DC, USA.

771 Berendse, F., Ruijven, J.V., Jongejans, E., Keesstra, S.D., 2015. Loss of Plant Species
772 Diversity Reduces Soil Erosion Resistance. *Ecosystems*. 18(5), 881-888. DOI:
773 10.1007/s10021-015-9869-6.

774 Bibalani, G.H., Majnonian, B., Adeli, E., Sanii, H., 2006. Slope stabilization with
775 *Gleditshia caspica* and *Parrotia persica*. *Int. J. Environ. Sci. Tech*. 2, 381-385.

776 Bonyad, A., 2006. Silvicultural Thinning Intensity Effects on Increasing the Growth of
777 Planted Loblolly Pine (*Pinus taeda* L.) Stands in Northern Iran, *Taiwan J For Sci*, 21(3),
778 317-26.

779 Burylo, M., Hudek, C., Rey, F., 2012. Plant root traits affecting the resistance of soils to
780 concentrated flow erosion. *Earth Surface Processes and Landforms*. 37, 1463-1470. Carter,
781 M.R., 2002. *Soil Quality for Sustainable Land Management: Organic Matter and*
782 *Aggregation Interactions that Maintain Soil Functions*. *Agron. J*. 94, 38–47.

783 Cerdà, A., González-Pelayo, O., Giménez-Morera, A., Jordán, A., Pereira, P., Novara, A.,
784 Brevik, E.C., Prosdocimi, M., Mahmoodabadi, M., Keesstra, S., García Orenes, F.,
785 Ritsema, C., 2016. The use of barley straw residues to avoid high erosion and runoff rates
786 on persimmon plantations in Eastern Spain under low frequency – high magnitude
787 simulated rainfall events. *Soil Research* 54, 154-165. DOI: 10.1071/SR15092.

788 David, D., 2000. Hydrologic effects of dryland shrubs: Defining the spatial extent of
789 modified soil water uptake rates at an Australian desert site. *Journal of Arid Environments*.
790 45, 159-172.

791 De Baets, S., Poeson, J., Reubens, B., Wemans, K., de Baer-demaeker, J., Muys, B., 2008.
792 Root tensile strength and root distribution of typical Mediterranean plant species and their
793 contribution to soil shear strength. *Plant and Soil*. 307, 207–226.

794 De Baets, S., Poesen, J., 2010. Empirical models for predicting the erosion-reducing effects
795 of plant roots during concentrated flow erosion. *Geomorphology*. 118, 425-432. DOI:
796 10.1016/j.geomorph.2010.02.011.

797 De Baets, S., Poesen, J., Gyssels, G., Knapen, A., 2006. Effects of grass roots on the
798 erodibility of topsoils during concentrated flow. *Geomorphology*. 76, 54–67.

799 De Baets, S., Poesen, J., Knapen, A., Galindo, P., 2007a. Impact of root architecture on the
800 erosion-reducing potential of roots during concentrated flow. *Earth Surf. Process. Landf. J.*
801 *Br. Geomorphol. Res. Group*. 32, 1323–1345.

802 De Baets, S., Poesen, J., Knapen, A., Barberá, G. G., & Navarro, J. A. (2007b). Root
803 characteristics of representative Mediterranean plant species and their erosion-reducing
804 potential during concentrated runoff. *Plant and Soil*, 294(1-2), 169-183.

805 De Leenheer, L. and De Boodt, M. 1959. Determination of aggregate stability by the change in mean weight
806 diameter. *Mededelingen van de Lundbouwhogeschool Gent*, 24, 290-300.

807 Durán, Z.V.H., Francia, M.J.R., Rodríguez, P.C.R., Martínez, R.A., Cárceles, R.B., 2006.
808 Soil erosion and runoff prevention by plant covers in a mountainous area (SE Spain):
809 implications for sustainable agriculture. *The Environmentalist*. 26, 309–319.

810 Ellison, W.D., 1947. Soil erosion studies: Part I. *Agric. Eng.* 28, 145–146.

811 Fiener, P., Auerswald, K., 2003. Effectiveness of grassed waterways in reducing runoff and
812 sediment delivery from agricultural watersheds. *Journal of Environmental Quality*. 32(3),
813 927-936.

814 Fortugno, D., Boix-Fayos, C., Bombino, G., Denisi, P., Quinonero Rubio, J. M.,
815 Tamburino, V., & Zema, D. A. (2017). Adjustments in channel morphology due to land-use
816 changes and check dam installation in mountain torrents of Calabria (southern Italy). *Earth*
817 *Surface Processes and Landforms* 42(14), 2469-2483.

818 Foster, G.R., 1982. Modeling the erosion process. In *Hydrologic Modeling of Small*
819 *Watersheds*; Haan, C.T., Ed.; ASAE: St. Joseph, MI, USA, pp. 296–380.

820 Foth, H.D., 1990. *Fundamentals of Soil Science*, 8th ed. John Wiley and Sons: New York,
821 NY, USA.

822 Geng, R., Zhang, G. H., Hong, D. L., Ma, Q. H., Jin, Q., & Shi, Y. Z. 2021. Response of
823 soil detachment capacity to landscape positions in hilly and gully regions of the Loess
824 Plateau. *Catena*, 196, 104852.

825 Gilman, E.F., Watson, D.G., 2014. *Parrotia persica*: Persian Parrotia. Environmental
826 Horticulture Department, Florida Cooperative Extension Service, Institute of Food and
827 Agricultural Sciences (IFAS), University of Florida, Gainesville FL 32611.

828 Google Earth V. 7.3.3.7786 (July 21, 2020). Saravan Forest Park, Iran.
829 37°08'10"N,49°40'18"E Eye alt. 916 m. DigitalGlobe 2020. <https://earth.google.com>
830 [November 28, 2020] Govers, G., Everaert, W., Poesen, J., Rauws, G., De Ploey, J.,
831 Lautridou, J.P., 1990. A long flume study of the dynamic factors affecting the resistance of
832 a loamy soil to concentrated flow erosion. *Earth Surf. Process. Landf.* 15, 313–328.

833 Grace III, J.M., 2002. Effectiveness of vegetation in erosion control from forest road
834 sideslopes. *Transactions of the ASAE. American Society of Agricultural Engineers.* 45 (3),
835 681–685.

836 Gupta, H.V., Sorooshian, S., Yapo, P.O., 1999. Status of automatic calibration for
837 hydrologic models: comparison with multilevel expert calibration. *J. Hydrol. Eng.* 4 (2),
838 135–143.

839 Gyssels, G., Poesen, J., 2003. The importance of plant root characteristics in controlling
840 concentrated flow erosion rates. *Earth Surf. Process. Landf.* 28, 371–384.

841 Gyssels, G., Poesen, J., Bochet, E., Li, Y., 2005. Impact of plant roots on the resistance of
842 soils to erosion by water: A review. *Prog. Phys. Geogr.* 29, 189–217.

843 Hacke, U.G., Sperry, J.S., Ewers, B.E., Ellsworth, D.S., Schäfer, K.V.R., Oren, R., 2000.
844 Influence of Soil Porosity on Water Use in *Pinus taeda*. *Oecologia* 124(4), 495-505.

845 Herbrich, M., Gerke, H.H., Sommer, M., 2018. Root development of winter wheat in
846 erosion-affected soils depending on the position in a hummocky ground moraine soil
847 landscape. *J. Plant Nutr. Soil Sci.* 181, 147-157.

848 Hosseini, S.M., 2003. Incomparable roles of Caspian forests: heritage of humankind. *Forest*
849 *Sci.*, 3, 31-40.

850 IRIMO (Islamic Republic of Iran Meteorological Organization), 2016. Annual Rainfall
851 Report. Available online: www.irimo.ir (accessed on 20 September 2019).

852 Jiao, J.Y., Tzanopoulos, J., Xofis, P., Mitchley, J., 2008. Factors affecting distribution of
853 vegetation types on abandoned cropland in the hilly-gullied Loess Plateau region of China.
854 *Pedosphere.* 18, 24-33.

855 Karimi, H.R., Sadeghi-Seresht, E., Nasrolahpour-Moghadam, S., Soleimani, S., Farahmand,
856 H., Jome-Yazdian, M.S., 2018. Effects Chemical Treatments and Stratification on
857 Seedlings Emergence of Persian Parrotia (*Parrotia Persica* (DC.) and Assessment of
858 Genetic Diversity in its Seedlings, *International Journal of Advanced Research in Botany*,
859 4(3), 1-15.

860 Kartoolinejad, D., Hosseini, S.M., Mirnia, S.K., Akbarinia, M., Shayanmehr, F., 2007. The
861 Relationship among Infection Intensity of *Viscum album* with some Ecological Parameters
862 of Host Trees, *Int. J. Environ. Res.*, 1(2), 143-149.

863 Keller, T., Håkansson, I., 2010. Estimation of reference bulk density from soil particle size
864 distribution and soil organic matter content. *Geoderma*, 154, 398-406.

865 Kervroëdan, L., Armand, R., Saunier, M., Ouvry, J.F., Faucon, M.P., 2018. Plant functional
866 trait effects on runoff to design herbaceous hedges for soil erosion control, *Ecological*
867 *Engineering*, 118, 143-151.

868 Khanal, A., Fox, G.A., 2017. Detachment characteristics of root-permeated soils from
869 laboratory jet erosion tests. *Ecological Engineering*. 100, 335-343.

870 Kooch, Y., Rostayee, F., Hosseini, S.M., 2016. Effects of tree species on topsoil properties
871 and nitrogen cycling in natural forest and tree plantations of northern Iran, *Catena*, 144, 65-
872 73.

873 Koskiaho, J., 2003. Flow velocity retardation and sediment retention in two constructed
874 wetland–ponds. *Ecological Engineering*. 19(5), 325-337.

875 Kottek, M., Grieser, J., Beck, C., Rudolf, B., Rubel, F., 2006. World Map of the Köppen-
876 Geiger climate classification updated. *Meteorol. Z.* 15, 259–263.

877 Krause, P., Boyle, D.P., Base, F., 2005. Comparison of different efficiency criteria for
878 hydrological model assessment. *Advances in Geosciences*. 5, 89-97.

879 Laflen, J.M., Lane, J.L., Foster, G.R., 1991. WEPP—A New Generation of Erosion
880 Prediction Technology. *J. Soil Water Cons.* 46 (1), 34-38.

881 Li, M., Hai, X., Hong, H., Shao, Y., Peng, D., Xu, W., Yang, Y., Zheng, Y., Xia, Z., 2019.
882 Modelling soil detachment by overland flow for the soil in the Tibet Plateau of China. *Sci.*
883 *Rep.* 9, 8063

884 Li, Y., Xu, X.-Q., Zhu, X.-M. and Tian, J-Y. 1992b. Effectiveness of plant roots on
885 increasing the soil permeability on the Loess Plateau. *Chinese Science Bulletin* 37, 1735–
886 38.

887 Li, Y., Xu, X.-Q. and Zhu, X.-M. 1993: Effective model on the roots of Chinese pine
888 plantation to improve the physical properties of soil in the Loess Plateau. *Scientia Silvae*
889 *Sinicae* 29, 193–98 (in Chinese).

890 Li, Y., 1995. *Plant Roots and Soils Anti-Scourability on the Chinese Loess Plateau* (in
891 Chinese). Beijing, China: Science Press.

892 Li, Y., Tang, C., Wang, C., Tian, W., Pan, B., Hua, L., Lau, J., Yu, Z., Acharya, K., 2013.
893 Assessing and modeling impacts of different inter-basin water transfer routes on Lake
894 Taihu and the Yangtze River, China. *Ecological engineering*. 60, 399-413.

895 Li, Y., Zhu, X.M., Tian, J.Y., 1991a. Benefits of vegetation roots to improve erodibility in
896 Loess Plateau (in Chinese). *Science Bulletin*. 36(12), 935-938.

897 Li, Y., Xu, X.Q., Zhu, X.M., 1992. Preliminary-study on mechanism of plant-roots to
898 increase soil antiscourability on the Loess Plateau. *Sci. China Ser. B-chem*. 35, 1085- 1092.

899 Li, Y., Zhu, X.M., Tian, J.Y., 1991b. Effectiveness of plant roots to increase the
900 antiscourability of soil on the Loess Plateau. *Chin. Sci. Bull*. 24, 2077- 2082.

901 Li, Z.W., Zhang, G.H., Geng, R., Wang, H., Zhang, X.C., 2015. Land use impacts on soil
902 detachment capacity by overland flow in the Loess Plateau, China. *Catena*. 124, 9–17.

903 Lu, J., Zhang, Q., Werner, A. D., Li, Y., Jiang, S., & Tan, Z. (2020). Root-induced changes
904 of soil hydraulic properties—A review. *Journal of Hydrology*, 125203.

905 Lucas-Borja, M.E., Zema, D.A., Carrà, B.G., Cerdà, A., Plaza-Alvarez, P.A., Cózar, J.S.,
906 de las Heras, J., 2018. Short-term changes in infiltration between straw mulched and non-
907 mulched soils after wildfire in Mediterranean forestland ecosystems. *Ecol. Eng*. 122, 27–
908 31.

909 Mamo, M., Bubenzer, G., 2001a. Detachment rate, soil erodibility, and soil strength as
910 influenced by living plant roots part I: laboratory study. *Trans. ASAE*. 44, 1167-1174.

911 Mamo, M., Bubenzer, G., 2001b. Detachment rate, soil erodibility, and soil strength as
912 influenced by living plant roots part II: field study. *Trans. ASAE*. 44, 1175-1181.

913 Mao, Z., Saint-Andre, L., Genet, M., Mine, F.X., Jourdan, C., Rey, H., Courbaud, B.,
914 Stokes, A., 2012. Engineering ecological protection against landslides in diverse mountain
915 forests: choosing cohesion models. *Ecological Engineering*. 45: 55–69.

916 Marvie-Mohadjer, M.R., 2019. *Silviculture*, 5th ed.; University of Tehran Press: Tehran,
917 Iran, p. 418.

918 Meek, B.D., Rechel, E.R., Carter, L.M., DeTar, W.R., Urie, A.L., 1992. Infiltration rate of
919 a sandy loam soil: Effects of traffic, tillage, and plant roots. *Soil Science Society of*
920 *America Journal*. 56, 908-913.

921 Mirabolfathy, M., Javad, A., Ashnaei, P., 2018. The occurrence of *Anthostoma decipiens*,
922 the causal agent of 'Carpinus betulus decline', in northern Iran, *New Disease Reports*, 37,
923 20. <http://dx.doi.org/10.5197/j.2044-0588.2018.037.020>.

924 Morgan, R., Quinton, J., Rickson, R., 1992. *EUROSEM: Documentation Manual*. Silsoe
925 College, Silsoe, UK.

926 Moriasi, D.N., Arnold, J.G., Van Liew, M.W., Bingner, R.L., Harmel, R.D., Veith, T.L.,
927 2007. Model evaluation guidelines for systematic quantification of accuracy in watershed
928 simulations. *Transactions of the ASABE*. 50 (3), 885-900.

929 Moriasi, D.N., Arnold, J.G., Van Liew, M.W., Bingner, R.L., Harmel, R.D., Veith, T.L.,
930 2007. Model evaluation guidelines for systematic quantification of accuracy in watershed
931 simulations. *Trans. ASABE*. 50, 885–900.

932 Nash, J.E., Sutcliffe, J.V., 1970. River flow forecasting through conceptual models part I-a
933 discussion of principles. *J. Hydrol.* 10, 282–290.

934 Nasiri, M., Zare, N., Jalilvand, H., 2012. Investigation of the effective factors on rate of
935 stemflow for tree species in Hyrcanian forests, *Egyptian Journal of Biology*, 14, 37-44.

936 Nearing, M.A.; Foster, G.R.; Lane, L.J.; Finkner, S.C. A process-based soil erosion model
937 for USDA-Water Erosion Prediction Project technology. *Trans. ASAE* 1989, 32, 1587–
938 1593.

939 Nearing, M.A., Bradford, J.M., Parker, S.C., 1991. Soil detachment by shallow flow at low
940 slopes. *Soil Sci. Soc. Am. J.* 55, 339–344.

941 Nearing, M.A., Foster, G.R., Lane, L.J., Finkner, S.C., 1989. A process-based soil erosion
942 model for USDA-Water Erosion Prediction Project technology. *Trans. ASAE*. 32, 1587–
943 1593.

944 Nearing, M.A., Norton, L.D., Bulgakov, D.A., Larionov, G.A., West, L.T., Dontsova,
945 K.M., 1997. Hydraulics and erosion in eroding rills. *Water Resour. Res.* 33, 865–876.

946 Nearing, M.A., Simanton, J.R., Norton, L.D., Bulygin, S.J., Stone, J., 1999. Soil erosion by
947 surface water flow on a stony, semiarid hillslope. *Earth Surf. Process. Landf.* 24, 677–686.

948 Norris, J. E., Di Iorio, A., Stokes, A., Nicoll, B. C., & Achim, A. (2008). Species selection
949 for soil reinforcement and protection. In *Slope stability and erosion control: ecotechnological solutions* (pp. 167-210). Springer, Dordrecht.

950

951 Owoputi, L., & Stolte, W. (1995). Soil detachment in the physically based soil erosion
952 process: a review. *Trans. ASAE*. 38 (4), 1099–1110.

953 Parhizkar, M., Shabanpour, M., Zema, D. A., & Lucas-Borja, M. E. (2020b). Rill Erosion
954 and Soil Quality in Forest and Deforested Ecosystems with Different Morphological
955 Characteristics. *Resources*, 9(11), 129.

956 Parhizkar, M., Shabanpour, M., Khaledian, M., Cerdà, A., Rose, C.W., Asadi, H., Lucas-
957 Borja, M.E., Zema, D.A., 2020a. Assessing and Modeling Soil Detachment Capacity by
958 Overland Flow in Forest and Woodland of Northern Iran. *Forests*. 11(1), 65.

959 Payam, H., Pourrajabali, S., 2020. Investigating the natural structures of *Quercus*
960 *castaneifolia* C.A.Meyer in managed tracks in connection with physiographic factors in
961 Northern Iran, *Acta Ecologica Sinica*, 40(2), 178-184.

962 Perez, J., Salazar, R. C., & Stokes, A. (2017). An open access database of plant species
963 useful for controlling soil erosion and substrate mass movement. *Ecological*
964 *Engineering*, 99, 530-534.

965 Picchio, R., Tavankar, F., Latterini, F., Jourgholami, M., Karamdost Marian, B., Venanzi,
966 R., 2020. Influence of Different Thinning Treatments on Stand Resistance to Snow and
967 Wind in Loblolly Pine (*Pinus taeda* L.) Coastal Plantations of Northern Iran, *Forests*,
968 11(10), 1034; <https://doi.org/10.3390/f11101034>.

969 Pollen, N., 2007. Temporal and spatial variability in root reinforcement of stream banks:
970 accounting for soil shear strength and moisture. *Catena*. 69, 197–205.

971 Polyakov, V.O., Nearing, M.A., 2003. Sediment transport in rill flow under deposition and
972 detachment conditions. *Catena*. 51, 33–43.

973 Prosdocimi, M., Cerdà, A., Tarolli, P., 2016. Soil water erosion on Mediterranean
974 vineyards: a review. *Catena*. 141, 1–21.

975 Querejeta, J. I., Roldán, A., Albaladejo, J., & Castillo, V., 2001. Soil water availability
976 improved by site preparation in a *Pinus halepensis* afforestation under semiarid
977 climate. *Forest Ecology and Management*, 149(1-3), 115-128.

978 Raei, B., Asadi, H., Moussavi, A., Ghadiri, H., 2015. A study of initial motion of soil
979 aggregates in comparison with sand particles of various sizes. *Catena*. 127, 279–286.

980 Rewald, B., & Rechenmacher, A., 2014. It's Complicated: Intraroot System Variability of
981 Respiration and Morphological Traits in Four Deciduous Tree Species. *Plant Physiol*. 166,
982 736-745.

983 Sagheb-Talebi, K.h., Sajedi, T., Yazdian, F., 2005. *Forests of Iran*. Research Institute of
984 Forests and Rangelands Publications, 2nd. Ed., 1-28.

985 Santhi, C., Arnold, J.G., Williams, J.R., Dugas, W.A., Srinivasan, R., Hauck, L.M., 2001.
986 Validation of the SWAT model on a large river basin with point and nonpoint sources. *J.*
987 *Am. Water Resour. Assoc.* 37 (5), 1169–1188.

988 Sefidi, K., Marvie Mohadjer, M.R., Etemad, V., Copenheaver, C.A., 2011. Stand
989 characteristics and distribution of a relict population of Persian ironwood (*Parrotia persica*
990 C.A. Meyer) in northern Iran, *Flora - Morphology, Distribution, Functional Ecology of*
991 *Plants.*, 206 (5), 418-422.

992 SDSD (Soil Science Division Staff), 2017. *Soil Survey Manual*; Ditzler, C., Scheffe, K.,
993 Monger, H.C., Eds.; USDA Handbook 18 Government Printing Office: Washington, DC,
994 USA.

995 Shabanpour, M., Daneshyar, M., Parhizkar, M., Lucas-Borja, M.E., Zema, D.A., 2020.
996 Influence of crops on soil properties in agricultural lands of northern Iran. *Science of The*
997 *Total Environment.* 711, 134694.

998 Shi, Z.H., Fang, N.F., Wu, F.Z., Wang, L., Yue, B.J., Wu, G.L., 2012. Soil erosion
999 processes and sediment sorting associated with transport mechanisms on steep slopes. *J.*
1000 *Hydrol.* 454, 123–130.

1001 Shinohara, Y., Otani, S., Kubota, T., Otsuki, K., Nanko, K., 2016. Effects of plant roots on
1002 the soil erosion rate under simulated rainfall with high kinetic energy. *Hydrological*
1003 *Sciences Journal.* 61 (13), 2435–2442.

1004 Singh, J., Knapp, H.V., Demissie, M., 2004. Hydrologic modeling of the Iroquois River
1005 watershed using HSPF and SWAT. ISWS CR 2004-08. Champaign, Ill. Illinois State Water
1006 Survey. <http://www.sws.uiuc.edu/pubdoc/CR/ISWSCR2004-08.pdf> (Accessed 14 February
1007 2018).

1008 Van Liew, M.W., Garbrecht, J., 2003. Hydrologic simulation of the Little Washita River
1009 experimental watershed using SWAT. *Journal of the American Water Resources*
1010 *Association.* 39, 413-426.

1011 Van Liew, M.W., Garbrecht, J., 2003. Hydrologic simulation of the Little Washita River
1012 experimental watershed using SWAT. *J. Am. Water Resour. Assoc.* 39, 413–426.

1013 Vannoppen, W., Vanmaercke, M., De Baets, S., Poesen, J., 2015. A review of the
1014 mechanical effects of plant roots on concentrated flow erosion rates. *Earth Sci. Rev.* 150,
1015 666–678

1016 Vannoppen, W., De Baets, S., Keeble, J., Dong, Y., & Poesen, J. (2017). How do root and
1017 soil characteristics affect the erosion-reducing potential of plant species?. *Ecological*
1018 *Engineering*, 109, 186-195.

1019 Vieira, D.C.S., Serpa, D., Nunes, J.P.C., Prats, S.A., Neves, R., Keizer, J.J., 2018.
1020 Predicting the effectiveness of different mulching techniques in reducing post-fire runoff
1021 and erosion at plot scale with the RUSLE, MMF and PESERA models. *Environmental*
1022 *Research*. 165, 365-378.

1023 Viles, H.A., 1990. The agency of organic beings: A selective review of recent work in
1024 biogeomorphology. In *Vegetation and Erosion: Processes and Environments*; Thornes, J.B.,
1025 Ed.; Wiley: Chichester, UK, pp. 5–25.

1026 Vogt, K. A., Vogt, D. J., Palmiotto, P. A., Boon, P., O'Hara, J., & Asbjornsen, H. (1995).
1027 Review of root dynamics in forest ecosystems grouped by climate, climatic forest type and
1028 species. *Plant and soil* 187(2), 159-219.

1029 Wang, B., Zhang, G.H., Zhang, X.C., Li, Z.W., Su, Z.L., Yi, T., Shi, Y.Y., 2014a. Effects
1030 of near soil surface characteristics on soil detachment by overland flow in a natural
1031 succession grassland. *Soil Sci. Soc. Am. J.* 78, 589–597.

1032 Wang, B., Zhang, G.H., Shi, Y.Y., Li, Z., 2015. Effects of Near Soil Surface Characteristics
1033 on the Soil Detachment Process in a Chronological Series of Vegetation Restoration. *Soil*
1034 *Science Society of America Journal*. 79(4), 1213-1222.

1035 Wang, B., Zhang, G.H., Yang, Y.F., Li, P.P., Liu, J.X., 2018b. The effects of varied soil
1036 properties induced by natural grassland succession on the process of soil detachment.
1037 *Catena*. 166, 192–199.

1038 Wang, B., Zhang, G.H., Shi, Y.Y., Zhang, X.C., 2014b. Soil detachment by overland flow
1039 under different vegetation restoration models in the Loess Plateau of China. *Catena*. 116,
1040 51–59.

1041 Wang, B., Zhang, G.H., Yang, Y.F., Li, F.F., Liu, J.X., 2018a. Response of soil detachment
1042 capacity to plant root and soil properties in typical grasslands on the Loess Plateau. *Agric.*
1043 *Ecosyst. Environ.* 266, 68–75.

1044 Wang, D.D., Wang, Z.L., Shen, N., Chen, H., 2016. Modeling soil detachment capacity by
1045 rill flow using hydraulic parameters. *J. Hydrol.* 535, 473–479.

1046 Wang, B., Li, P. P., Huang, C. H., Liu, G. B., & Yang, Y. F. Effects of root morphological
1047 traits on soil detachment for ten herbaceous species in the Loess Plateau. *Science of the*
1048 *Total Environment*, 754, 142304.

1049 Wang, D.D.; Wang, Z.L.; Shen, N.; Chen, H. Modeling soil detachment capacity by rill
1050 flow using hydraulic parameters. *J. Hydrol.* 2016, 535, 473–479.

1051 Xiao, H., Liu, G., Liu, P.L., Zheng, F.L., Zhang, J.Q., Hu, F.N., 2017. Response of soil
1052 detachment rate to the hydraulic parameters of concentrated flow on steep loessial slopes on
1053 the loess plateau of China. *Hydrol. Process.* 31, 2613–2621.

1054 Yang, C.T., 1972. Unit stream power and sediment transport. *J. Hydrol. Div. ASCE.* 98,
1055 1805–1826.

1056 Yang, B., Lee, D.K., Heo, H.K., Biging, G., 2019. The effects of tree characteristics on
1057 rainfall interception in urban areas, *Landscape and Ecological Engineering*, 15, 289–296.

1058 Zema, D.A., Bingner, R.L., Govers, G., Licciardello, F., Denisi, P., Zimbone, S.M., 2012.
1059 Evaluation of runoff, peak flow and sediment yield for events simulated by the AnnAGNPS
1060 model in a Belgian agricultural watershed. *Land Degradation and Development* 23(3), 205-
1061 215. <https://doi.org/10.1002/ldr.1068>.

1062 Zhang, G.H., Tang, K.M., Ren, Z.P., Zhang, X.C., 2013. Impact of grass root mass density
1063 on soil detachment capacity by concentrated flow on steep slopes. *Trans. ASABE* 56, 927–
1064 934.

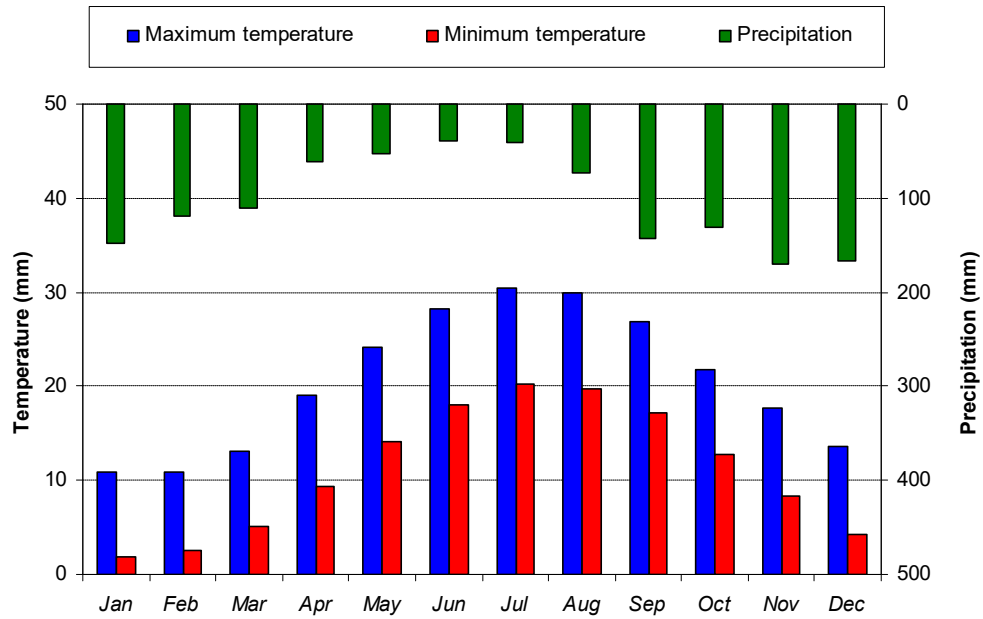
1065 Zhang, G.H., Liu, B.Y., Liu, G.B., He, X.W., Nearing, M.A., 2003. Detachment of
1066 undisturbed soil by shallow flow. *Soil Sci. Soc. Am. J.* 67, 713–719.

1067 Zhang, G.H., Liu, B.Y., Nearing, M.A., Huang, C.H., Zhang, K.L., 2002. Soil detachment
1068 by shallow flow. *Trans. ASAE.* 45, 351–357.

1069 Zhang, G.H., Liu, G.B., Tang, K.M., Zhang, X.C., 2008. Flow detachment of soils under different land uses in
1070 the Loess Plateau of China. *Trans. ASABE.* 51, 883–890.

1071 **SUPPLEMENTARY DATA**

1072



1073

1074 Figure 1(SD) – Mean values of monthly temperature and precipitation measured at the
1075 nearest meteorological station (records of the last 20 years) in Saravan Forest Park (Iran).

1076 Table 1(SD) - Flow characteristics in the experiments carried out for measuring the rill detachment capacity under four tree species in Saravan
 1077 Forest Park (Northern Iran).
 1078

Experiment	S [m m ⁻¹]	q [L m ⁻¹ s ⁻¹]	h [m]	R [m]	V [m s ⁻¹]	τ [Pa]	Ω [kg s ⁻³]	ω [m s ⁻¹]	D_c [kg s ⁻¹ m ⁻²]			
									<i>C. betulus</i>	<i>Q. castaneifolia</i>	<i>P. taeda</i>	<i>P. persica</i>
1	0.01	0.26	0.006	0.005	0.09	0.51	0.04	0.001	0.00001	0.00004	0.00006	0.00009
2		0.35	0.007	0.006	0.14	0.59	0.08	0.001	0.00003	0.00007	0.00009	0.00010
3		0.46	0.009	0.008	0.19	0.76	0.14	0.002	0.00005	0.00009	0.00015	0.00016
4		0.57	0.010	0.009	0.26	0.89	0.23	0.003	0.00006	0.00011	0.00017	0.00019
5		0.69	0.012	0.011	0.31	1.05	0.32	0.003	0.00008	0.00013	0.00015	0.00027
6	0.02	0.26	0.005	0.004	0.13	0.88	0.11	0.003	0.00011	0.00022	0.00034	0.00039
7		0.35	0.006	0.005	0.19	1.07	0.20	0.004	0.00027	0.00038	0.00047	0.00059
8		0.46	0.008	0.007	0.25	1.36	0.34	0.005	0.00044	0.00057	0.00066	0.00077
9		0.57	0.009	0.008	0.31	1.55	0.48	0.006	0.00062	0.00069	0.00078	0.00089
10		0.69	0.011	0.010	0.36	1.94	0.69	0.007	0.00086	0.00091	0.00099	0.00150
11	0.03	0.26	0.004	0.004	0.19	1.07	0.20	0.006	0.00100	0.00160	0.00190	0.00250
12		0.35	0.005	0.005	0.23	1.42	0.32	0.007	0.00130	0.00190	0.00290	0.00360
13		0.46	0.007	0.006	0.29	1.79	0.52	0.009	0.00160	0.00220	0.00350	0.00390
14		0.57	0.008	0.007	0.37	2.12	0.78	0.011	0.00190	0.00240	0.00370	0.00410

15		0.69	0.010	0.009	0.42	2.67	1.12	0.013	0.00230	0.00260	0.00390	0.00440
16	0.04	0.26	0.003	0.003	0.21	1.10	0.29	0.011	0.00320	0.00340	0.00430	0.00480
17		0.35	0.004	0.004	0.31	1.43	0.44	0.012	0.00350	0.00370	0.00470	0.00510
18		0.46	0.005	0.005	0.37	1.83	0.67	0.015	0.00380	0.00420	0.00490	0.00530
19		0.57	0.007	0.006	0.42	2.46	1.03	0.017	0.00420	0.00460	0.00550	0.00560
20		0.69	0.009	0.008	0.46	3.07	1.41	0.018	0.00440	0.00490	0.00570	0.00590
21	0.05	0.26	0.002	0.002	0.32	1.14	0.36	0.016	0.00490	0.00540	0.00590	0.00620
22		0.35	0.003	0.003	0.36	1.47	0.53	0.018	0.00510	0.00560	0.00620	0.00640
23		0.46	0.004	0.004	0.41	1.97	0.81	0.021	0.00540	0.00590	0.00650	0.00670
24		0.57	0.006	0.006	0.46	2.90	1.33	0.023	0.00560	0.00620	0.00670	0.00690
25		0.69	0.007	0.006	0.51	3.12	1.59	0.026	0.00580	0.00650	0.00740	0.00770

1079 Notes: D_c = rill detachment capacity; h = flow depth; R = hydraulic radius; q = flow rate per unit width; S = slope gradient; V = average water flow velocity; τ = hydraulic shear
1080 stress; ω = unit stream power; Ω = stream power.

1081